2019 Fall Semester MSE Ph. D. Qualifying Exam
(Polymer Characterization)

Date:
Professor: Dr. Donglu Shi Qualifier Committee Chair

Important Notes:

- No late exam submission will be accepted
- Put only the Qualifying Exam Number (QE#) on ALL sheets of paper related to the exam
- Put page number at the bottom center on ALL sheets of paper related to the exam
- Neatly display all pertinent diagrams, equations, etc. to illustrate a fully developed solution to the problem. *Points will be deducted for illegible work.*

QE number

1a. Using appropriate equations and sketches, briefly discuss what you understand by the terms, “glass-rubber transition and glass transition temperature”, Tg of a polymer and describe the factors that affect the Tg of a polymer.

1b. List three methods that can be used to measure the Tg of a polymer and rank these methods according to their accuracy for measuring Tg. In each case indicate what changes are occurring during the measurement and how these changes enable one to obtain the Tg of the polymer.

1c. Using suitable equations and sketches describe how the differential scanning calorimetry can be used to determine the Tg of isotactic polypropylene, iPP. In your answer state (i) the equipment to used, (ii) the procedure to be followed, (iii) the nature of the data obtained, (iv) how the Tg of iPP is obtained from your data.

2. The Fourier Transform (FT) involves deconvolution of a summation of sin waves from a decay or noise pattern. In polymer characterization the FT is used in FTIR, NMR, and in diffraction/scattering making it a common mathematical tool for characterization.

a) Explain how a FT could be used to understand variation in the Dow Jones average with time. The DJ average is an average of the top 500 stock prices on the New York Stock Exchange.

b) Describe an interferometer by sketching the device and the interferogram that results. How is a FT used with the interferogram?

c) How is an interferometer used in an FTIR? What component does it replace compared to a dispersive IR instrument?

d) How are FTs used in NMR? Explain what δ is in an NMR data plot.

e) In scattering, the scattering vector, $|\boldsymbol{q}| = 4\pi/\lambda \sin \theta$, is used to describe the spatial period of density oscillations, $d = 2\pi/|\boldsymbol{q}|$. How is a FT used to relate real space (d-space) and inverse space (q-space) in scattering/diffraction?

2019 Fall Semester MSE Ph. D. Qualifying Exam
(Polymer Physics)

Date:
Professor: Dr. Donglu Shi Qualifier Committee Chair

Important Notes:

- No late exam submission will be accepted
- Put only the Qualifying Exam Number (QE#) on ALL sheets of paper related to the exam
- Put page number at the bottom center on ALL sheets of paper related to the exam
- Neatly display all pertinent diagrams, equations, etc. to illustrate a fully developed solution to the problem. *Points will be deducted for illegible work.*

QE number

1. S Chandran et al. (*Processing Pathways Decide Polymer Properties at the Molecular Level* Macromolecules 2019 DOI: 10.1021/acs.macromol.9b01195) discuss the general problem of linking molecular orientation during processing with properties in processed polymers. They choose three types of processing: spin coating, stretched polymer fibers, and flow-induced crystallized polymers.

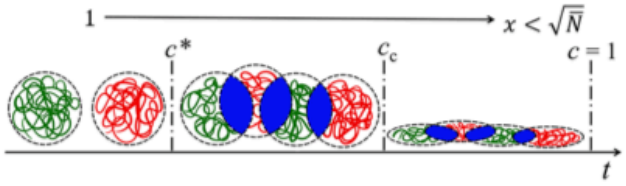

Figure 1. From isolated polymer coils to glassy polymers: In the course of evaporation, the initially separated polymers in a dilute

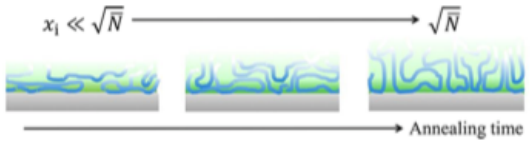

Figure 2. Equilibrating polymer conformations at an adsorbing interface: Schematic illustration of possible variations in polymer conformations at the substrate interface as a function of annealing time at temperatures $T > T_g$, where T_g is the glass transition temperature. Immediately after spin coating, polymers at the interface

a) Figure 1 shows Chandran et al.'s impression of a polymer that dries on a surface from a solution. Concentration increases during drying. Explain the transition between the first and second cartoon. Define c^* and explain how you think it would impact the chain structure during drying. Would you expect a difference in surface tension between the left and center solutions in Figure 1?

b) The second to third cartoon in Figure 1 relates to a transition in chain dynamics. Sketch a plot of log of the zero-shear rate viscosity versus log of the shear rate for a high molecular weight polymer melt and identify the dynamic relaxation time. Show how the shape of this curve would change with dilution. And use these viscosity curves to explain the meaning of c_e in Figure 1.

c) Explain the origin of the term √N in Figure 1.

d) In Figure 2, x is the number of interpenetrating chains at the substrate interface. Why is this value important and what is the relevance of $\sqrt{N}$ to this value?

e) Paint is partially a polymer in a solvent that is applied under shear to a surface. From your answers to parts a to d, explain the final polymer conformation you would expect in the dried paint. How would this conformation impact the performance of the paint?

2. Polymer networks and elastomers are normally produced by introduction of a crosslinking agent such as elemental sulfur into a polymer melt containing reactive functional groups such as double bonds in polybutadiene. Reaction leads to multifunctional crosslink sites that produce a molecular network so that the entire sample is a single molecule. Single chain nanoparticles (SCPNs) are chains that are crosslinked within a single chain, intrachain crosslinking, but not between different chains, interchain crosslinking, as in a rubber. Arbe et al. (*Mesoscale Dynamics in Melts of Single-Chain Polymeric Nanoparticles* Macromolecules 2019, 52, 6935-3942.) reports on studies of melts of such SCPNs.

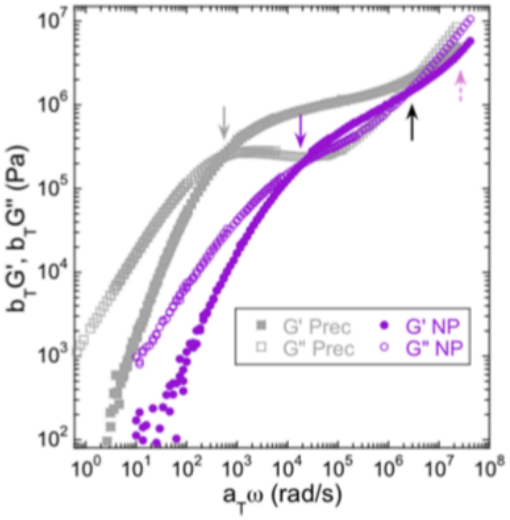

Figure 5. Rheological master curves (reference temperature 293 K).

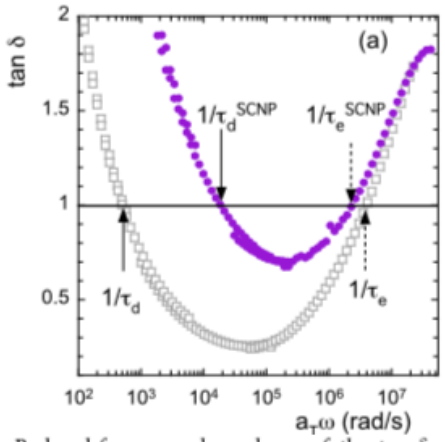

Figure 6. Reduced-frequency dependence of the tan $\delta = G''(\omega)/G'(\omega)$ corresponding to the rheological master curves shown in Figure 5 (empty squares, precursor; filled circles, SCNPs). (a) Results in a wide frequency range, while (b) blows up of the high-frequency region.

a) Figure 5 shows the dynamic rheology curves for an SCPN and the linear chain from which it was made (Precursor or "Prec" in the graph). Define G'', G', and tan δ.

b) In Figure 6, what does a value of tan $\delta > 1$ mean in terms of the material properties.

c) In Figure 6, explain how a transition from tan $\delta > 1$ to tan $\delta < 1$ can occur with a change in frequency.

d) In Figure 6, what are the meanings of τ_d and τ_e?

e) Why would τ_d be significantly different between the linear and SCPN samples while τ_e is comparable between the two samples?

Macromolecules

Perspective

Cite This: Macromolecules XXXX, XXX, XXX−XXX

pubs.acs.org/Macromolecules

Processing Pathways Decide Polymer Properties at the Molecular Level

Sivasurender Chandran,[*,†] Jörg Baschnagel,[‡] Daniele Cangialosi,[§,∥] Koji Fukao,[⊥] Emmanouil Glynos,[#] Liesbeth M. C. Janssen,[%] Marcus Müller,[&] Murugappan Muthukumar,[@] Ullrich Steiner,[△] Jun Xu,[□] Simone Napolitano,[*,○] and Günter Reiter[*,†]

[†]Institute of Physics, University of Freiburg, Freiburg 79104, Germany

[‡]Institut Charles Sadron, Université de Strasbourg & CNRS, 23 rue du Loess, 67034 Cedex, Strasbourg, France

[§]Centro de Física de Materiales CFM (CSIC-UPV/EHU) and Materials Physics Center MPC, Paseo Manuel de Lardizabal 5, 20018 San Sebastián, Spain

[∥]Donostia International Physics Center (DIPC), Paseo Manuel de Lardizabal 4, 20018 San Sebastin, Spain

[⊥]Department of Physics, Ritsumeikan University, Kusatsu, Shiga 525-8577, Japan

[#]Institute of Electronic Structure and Laser, Foundation for Research and Technology-Hellas, P.O. Box 1385, 711 10 Heraklion, Crete, Greece

[%]Theory of Polymers and Soft Matter, Department of Applied Physics, Eindhoven University of Technology, P.O. Box 513, 5600MB Eindhoven, The Netherlands

[&]Institute for Theoretical Physics, Georg-August-Universität, Göttingen, Germany

[@]Department of Polymer Science and Engineering, University of Massachusetts, Amherst, Massachusetts 01003, United States

[△]Adolphe Merkle Institute, Chemin des Verdiers 4, 1700 Fribourg, Switzerland

[□]Advanced Materials Laboratory of Ministry of Education, Department of Chemical Engineering, Tsinghua University, Beijing 100084, China

[○]Laboratory of Polymer and Soft Matter Dynamics, Experimental Soft Matter and Thermal Physics, Faculté des Sciences, Université libre de Bruxelles (ULB), CP223, Boulevard du Triomphe, Bruxelles 1050, Belgium

ABSTRACT: Conditions of rapid processing often drive polymers to adopt nonequilibrium molecular conformations, which, in turn, can give rise to structural, dynamical, and mechanical properties that are significantly different from those in thermodynamic equilibrium. However, despite the possibility to control the desired nonequilibrium properties of polymers, a rigorous microscopic understanding of the processing−property relations is currently lacking. In an attempt to stimulate progress along this topical direction, we focus here on three prototypical and apparently different cases: spin-coated polymer films, rapidly drawn polymer fibers, and sheared polymer melts. Inspired by the presence of common observations in the chosen cases, we search for order parameters as, for example, topological correlations and heterogeneities, which may allow characterizing the processing-induced behavior of polymers. We highlight that such approaches, necessitating concerted efforts from theory, simulations, and experiments, can provide a profound understanding leading to predictable and tunable properties of polymers.

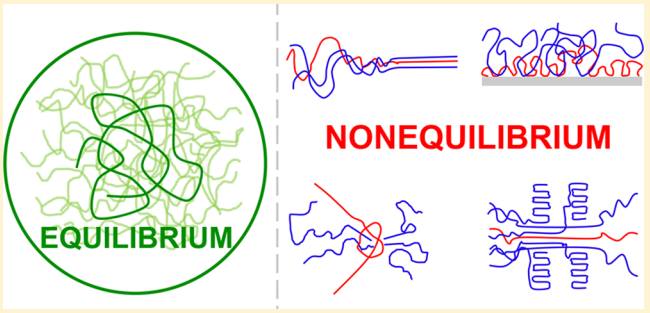

INTRODUCTION

Polymers are an important class of materials with an ever-growing market.[1,2] Their low cost, ease of processing, and broadly tunable properties are key reasons underlying their tremendous applicability, ranging from ordinary household items and packaging materials to high-tech fibers, medical devices, and wearable electronics. For most purposes, and most fabrication protocols, polymers are processed at rates much higher than the inverse of the equilibration time, i.e., the reptation time.[3−7] While the reptation time might be the longest relaxation time of individual entangled polymers, collective behavior and structure formation processes may involve time scales that are orders of magnitude longer. As a consequence, polymers (in melts and in solutions) often fail to

Received: June 11, 2019
Revised: August 7, 2019

DOI: 10.1021/acs.macromol.9b01195
Macromolecules XXXX, XXX, XXX−XXX

equilibrate on the time scale of a typical processing experiment, causing the macromolecules to freeze into nonequilibrium conformations. For example, rapid quenching can effectively reduce the rotational degrees of freedom of polymer chains; this, in turn, can give rise to structural, dynamical, and mechanical material properties that differ strongly from those in thermodynamic equilibrium. Nonequilibrium processing, i.e., processing under conditions that do not allow for equilibration, can thus offer a practical means to extend the range of available properties for a given material composition, holding enormous application potential for the development of novel material functionalities. However, despite the exciting possibility to control the molecular configuration space and resultant material properties directly by the processing protocol, a rigorous understanding of the processing−property relations of polymers is still lacking.

Recent experiments,[4−36] reflecting conditions also relevant in industrial processing of polymers, provide intriguing observations, which add to the feasibility of designing macroscopic properties of polymers via nonequilibrium processing: (1) The extent of deviations from equilibrium conformations[37] increases with increasing processing rates, implying that the nonequilibrium nature of the material can be directly controlled by the processing time scale. (2) After processing, the system tends to attain a conformation that minimizes the free energy. However, this equilibration kinetics is often so slow that one can harness the desired nonequilibrium deviation over time scales longer than those of technological interest. Following such strategies, it is thus possible to tune properties such as mechanical strength,[10−17] thermal expansion,[23,27] thermal conductivity,[35] and viscosity[10,13,15] by designing appropriate nonequilibrium processing protocols. (3) The above observations hold true for various geometries, ranging from bulk to nanoconfined systems. Importantly, such processing-induced nonequilibrium conformations have also resulted in novel applications. For example, polyethylene fibers composed of highly stretched molecules, whose conformations strongly deviate from those at equilibrium, show extremely high mechanical strength, enabling various uses ranging from bulletproof vests to cables for towing ships.[4,34] Despite such enormous application potential, the current state-of-the-art relies on empirical relations for obtaining desired properties. In order to controllably target specific material structures and functionalities, new concepts must be developed that directly relate processing protocols to the molecular nonequilibrium conformations and resultant macroscopic polymer properties.

The purpose of this article is to guide and stimulate discussion on the design, synthesis, processing, and characterization of novel polymeric materials. In particular, our long-term goal is to generate a fundamental understanding providing answers to the following questions: (1) What are the relevant molecular parameters that describe the nonequilibrium state of a processed material? (2) How do processing conditions affect material properties; that is, how does the macromolecular structure affect the magnitude and lifetime of deviations in chain conformations? (3) How can we design materials with desired properties via nonequilibrium processing pathways? To address these questions, among the virtually endless number of nonequilibrium processing pathways, we focus here on three prototypical and *apparently* different cases: spin-coated polymer films, rapidly drawn polymer fibers, and sheared polymer melts. Our choice of these three cases allows us to discuss various phenomena, like the deformation of polymers, reduced entanglement density, structure formation, and crystallization at conditions far from equilibrium, which are essential to various industrial processing techniques like injection stretch blow molding of plastic bottles and gel electrospinning of polymer fibers. Inspired by the existence of common features in various nonequilibrium processing pathways, we search for order parameters characterizing the behavior of polymers induced through processing. We highlight how the concerted effort from theory, simulations, and experiments on polymers at controlled nonequilibrium processing conditions can provide a profound understanding leading to predictable and tunable properties.

KEY EXPERIMENTAL OBSERVATIONS

Spin-Coated Polymer Films. Spin coating is a widely employed method to fabricate smooth polymer films of precisely controllable thickness, even in the nanometer range. Briefly, the technique amounts to depositing a polymer solution onto a flat surface, which is then rotated at high speed to spread the solution by centrifugal force. At the same time the solvent is rapidly evaporated—a key process that induces a transition to a dry polymer film. Polymer conformations are subjected to significant changes while going from separated polymer coils dispersed in the solvent (prior to spin coating) to a condensed phase upon vitrification (a few seconds later) (Figure 1). In the course of solvent evaporation, coils begin to overlap and to entangle. One might expect that at the end of this process the entanglement density would reach the equilibrium value typical of polymer melts. However, various experiments suggest that this is not the case.[8−17,19]

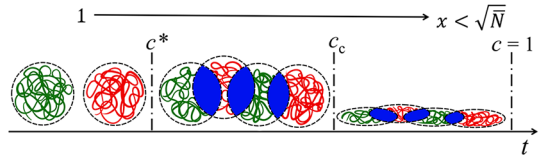

Figure 1. From isolated polymer coils to glassy polymers: In the course of evaporation, the initially separated polymers in a dilute solution begin to overlap, at a concentration[37] $c^* \sim N/V_e$ (where V_e is the envelope volume of the polymer consisting of N monomers), then interpenetrate, and entangle with each other. Above a threshold concentration c_c, the relaxation time of polymers becomes so high that their dynamics is frozen.[16] Continued evaporation induces a deformation of coils along the z-direction. Finally, at $c = 1$, we obtain dry glassy polymer films, with only partially interpenetrating polymers with $x < \sqrt{\bar{N}}$, where x is the number of interpenetrating chains in a freshly spin-coated film and $\bar{N}$ is the invariant degree of polymerization, characterizing the number of neighboring chains contained within the envelope volume of a reference chain.[38] Different colors were chosen to distinguish neighboring coils and emphasize overlapping regions. Reproduced with permission from ref 18.

As long as sufficiently many solvent molecules are present in the film, polymers will be able to relax and fully equilibrate. However, upon evaporation, the relaxation time of polymers progressively increases, inducing a "self-retardation" effect. Eventually, the structural relaxation time of the polymer chain will become longer than the time needed to evaporate the remaining solvent molecules, thus making equilibration effectively impossible. For some vitrifying polymers, this may occur even at polymer concentrations of the order of 50%.

DOI: 10.1021/acs.macromol.9b01195
Macromolecules XXXX, XXX, XXX−XXX

Evaporating the still remaining solvent molecules from this glassy polymer film will induce molecular deformations leading to stresses within the film. It is likely that such nonequilibrated coils interpenetrate only partially, in contrast to equilibrated polymers. In the latter case, one expects an average of $\sqrt{N}$ interpenetrating chains (neglecting prefactors) within the envelope volume V_e of a polymer;[37] a rapidly spin-coated film is expected to exhibit a far lower degree of interpenetration ($x \ll \sqrt{N}$, Figure 1). We anticipate that the ratio $x/\sqrt{N}$ may serve as one order parameter characterizing some aspects of the nonequilibrium polymer conformations and concomitant correlations in freshly spin-coated polymer films. Importantly, the nonequilibrium molecular conformations achieved upon the rapid removal of solvent can give rise to in-plane tensile stresses, which are related to the experimentally measured preparation-induced residual stresses.[8−12,15−17] Hence, by exploiting the competition between solvent evaporation and polymer relaxation—and thus the extent of deviations from equilibrium—it becomes possible to directly tune the mechanical properties of the film. Indeed, by using for example films obtained at different evaporation rates,[16,17] one can vary the residual stresses by several orders of magnitude. The degree of observed nonequilibrium dynamics, as encoded in the residual stresses and the corresponding (long) relaxation times, can also be associated with a dimensionless "processing parameter", which is defined by the ratio of the time scale of molecular relaxation to evaporation time.[16−18] This parameter, analogous to the Deborah number or the Weissenberg number, thus offers a practical means to quantitatively control the degree of nonequilibrium, and the resulting mechanical properties of the material, directly via the processing protocol.

Future efforts from simulations and theory may help to understand the microscopic mechanisms underlying deviations from equilibrium caused by preparation-induced residual stresses. These studies should also take into account the vast number of experiments performed on spin-coated polymer films, which have revealed a large number of intriguing properties induced by preparation. For example, the glass transition temperature T_g of these films shows changes by 10−50 K,[39−41] which may translate to changes in the relaxation time by several orders of magnitude. In fact, experiments[42−45] yield a broad distribution of relaxation times in spin-coated polymer films, suggesting temporal and spatial variations in polymer dynamics and, possibly, differences in local structures. Can we relate these intriguing observations with processing-induced changes in properties? A series of recent experiments demonstrate that the extent of deviations in T_g decreases upon annealing films at a temperature $T > T_g$ for times much longer than the time scales associated with the relaxation of equilibrated polymer melts,[21,22,41,46] highlighting the metastable character of the observed deviations. Interestingly, variations in T_g with changes in annealing time are attributed to concomitant changes in the extent of polymer adsorption to the substrate. This, in turn, is related to the equilibration of the whole spin-coated film, which is facilitated via concerted rearrangements of a few segments.[18,47] Such rearrangements increase the number of interpenetrating chains at the interface (and in the bulk) to approach the equilibrium value of $\sqrt{N}$ (Figure 2), corresponding to an increase in the number of chains adsorbed per unit surface.[48] We argue that a better understanding of the link between this molecular picture and the emergent macroscopic mechanical properties will be key in designing and optimizing new processing pathways to harness nonequilibrium behavior for the development of novel functional materials.

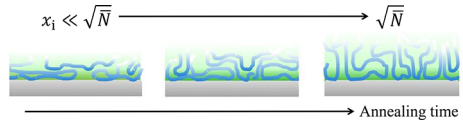

Figure 2. Equilibrating polymer conformations at an adsorbing interface: Schematic illustration of possible variations in polymer conformations at the substrate interface as a function of annealing time at temperatures $T > T_g$, where T_g is the glass transition temperature. Immediately after spin coating, polymers at the interface are frozen with rather flat conformations and hence exhibit a reduced interpenetration with other chains at the interface ($x_i \ll \sqrt{N}$, where x_i is the number of interpenetrating chains at the substrate interface in a freshly spin-coated film). Upon annealing, changes in conformation and further adsorption are only possible by the reorganization of already adsorbed chains, which is a possible reason behind the observation that equilibrium ($x \sim \sqrt{N}$) is only possible for annealing times that are much longer than the time scale associated with the relaxation of equilibrated melts.[37] Reproduced with permission from ref 21. Copyright 2011 Nature Publishing Group.

Highly Stretched Polymer Fibers. Polymer fibers, consisting of stretched and aligned chains, and their enhanced mechanical properties represent a trademark example for "processing pathways deciding polymer properties".[4,34,49−51] The essential step here is to stretch polymers to their full extension, such that the macroscopic material properties strongly differ from those in equilibrium. The chain extension can be characterized by the maximum draw ratio at a molecular level, $\lambda_{max} \sim \frac{N}{\sqrt{N}}$.[52] In practice, the draw ratio λ is defined as the ratio of the final to the initial length of the macroscopic sample.[49] Various techniques including gel spinning, electrospinning, and melt spinning have been developed for achieving high draw ratios and high elongational stresses in order to increase the extent of polymer stretching.[4,34,49,50,53] In addition, such strong stretching of polymers significantly affects structure formation of crystallizable polymers, which decides their macroscopic properties.[4,29,34] Fibers of polyethylene obtained at a draw ratio of around 100 have yielded an elastic modulus of ≈ 200 GPa, i.e., a factor of 300 higher than the Young's modulus of polyethylene in the bulk.[4,34] Importantly, the specific strength, i.e., the tensile strength normalized by mass density, of such commercially available polyethylene fibers is a factor of around 10 higher than that of stainless steel.[4] Currently, our understanding of these observations is largely empirical.[4,34] Unfortunately, such empirical relations lack connections to the underlying processing-induced nonequilibrium conformations, hampering progress in the rational design of fully optimized processing pathways. For instance, if we were able to generalize and translate processing strategies, which have been successful in gel spinning/electrospinning of polymer fibers, to other polymeric products, we may anticipate advancements in various technologies, for example, through mechanically resilient yet lightweight materials. In analogy to the spin-coated polymer films discussed above, in which the processing parameter is defined by the ratio of the evaporation time to the time characterizing the intrinsic dynamics, the fabrication of highly stretched fibers can also be characterized by dimensionless processing parameters.[50,53] Such parameters

DOI: 10.1021/acs.macromol.9b01195
Macromolecules XXXX, XXX, XXX−XXX

validate our central hypothesis that quantitative experiments performed under controlled nonequilibrium conditions provide strategies to design properties of polymers at the molecular level.

Flow-Induced Crystallization of Polymers. During processing, the application of large shear or extensional flow rates will stretch and align polymers with respect to the flow direction (Figure 3). As these aligned polymers lack positional

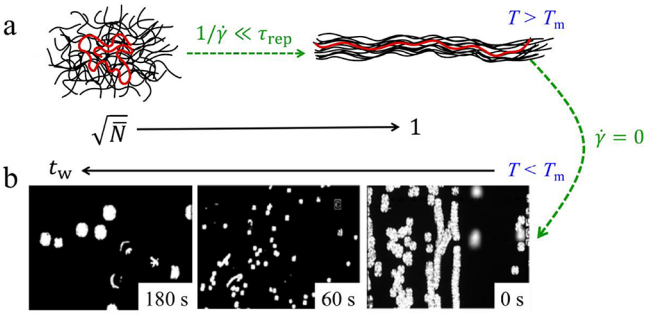

Figure 3. Stretching polymer chains and its consequence on crystallization: (a) Schematic illustration of flow-induced stretching of polymers, where a transition from equilibrium interpenetration to no interpenetration of a test chain (shown in red) with neighboring chains (shown in black) is depicted. (b) Optical micrographs capturing the influence of the state of the initial melt on the resulting nucleation density of isotactic polystyrene crystals obtained at 180 °C. Prior to crystallization, the sample was sheared at 250 °C for 10 s at a shear rate of $\dot{\gamma} = 30\ s^{-1}$ followed by waiting for different times t_w at 250 °C, as indicated in the figure. The nominal melting point of isotactic polystyrene is $T_m = 230$ °C. Micrographs are adapted from ref 31.

long-range order, the local molecular structure resembles those of nematic liquid crystals.[54−57] Even after the cessation of flow, it takes extraordinarily long waiting times for polymers to equilibrate, i.e., to change from processing-induced non-interpenetrating chains to the equilibrium entanglement density (Figure 3a). Such long-living memory effects are often dubbed as flow-induced memory. Interestingly, even at relatively high temperatures above the nominal melting temperature T_m, experiments reveal the presence of flow-induced structures.[29,31,32,58] After subsequent cooling to $T < T_m$, these aligning chains are found to ease nucleation and, hence, accelerate the crystallization kinetics (Figure 3b). Remarkably, crystals formed by cooling of flow-induced precursors exhibit morphologies otherwise not achievable from an equilibrated melt. Various continuum approaches[59−62]—based on Schneider rate equations—have been proposed to model such flow-induced changes in the crystallization kinetics. However, these macroscopic models cannot predict the nucleation rate for a given chain deformation but rather require this as an input for modeling (see the review by Graham for more details[62]). In addition, the absence of molecular details severely limits their applicability to understand various intriguing processing-induced observations. For instance, complementary experiments[31] show that the lifetime of flow-induced precursors increases rapidly upon decreasing temperature, yielding high activation energies. Such an increase in activation energy is commonly associated with a cooperative motion of segments—a condition expected for aligned segments of flow-induced precursors. A large degree of alignment among polymer chains might also be formed under other processing conditions. High flow rates can, for example, also be obtained when polymers slip rapidly on solid substrates, as in the case of dewetting.[15] Thus, we expect the occurrence of flow-induced polymer alignment during dewetting of thin polymer films at $T > T_m$. Indeed, recent dewetting experiments on isotactic polystyrene[15] show a temperature-dependent shear thickening behavior, accompanied by a relatively high activation energy. Both features hint at the presence of flow-induced structures. Importantly, in contrast to isotactic polystyrene, atactic polystyrene—polystyrene with irregularly arranged side groups—does not show high activation energies. Thus, it seems possible to harness the viscoelastic response of polymers by dialing in a certain regularity in the arrangement of side groups and by controlling the flow conditions during processing.

The experimental observations described above clearly demonstrate that rapid processing conditions, inducing significant changes in molecular conformations, play a key role in determining various macroscopic properties of polymers. Many of these so improved properties cannot be achieved from equilibrated polymer melts. Interestingly, nonequilibrated polymers obtained via different processing pathways exhibit dynamics of correlated polymers varying locally in space and time. The presence of common features in different experiments, such as the topological correlations between segments and the transition from $\sqrt{N}$ interpenetrating chains in equilibrium to no interpenetration between the

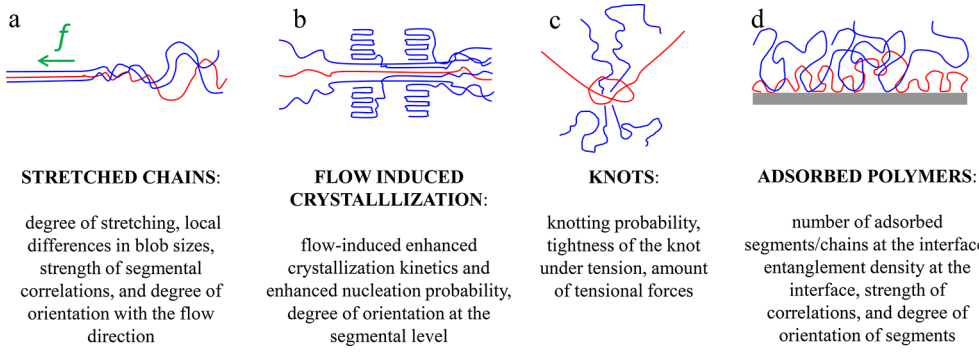

Figure 4. Representative nonequilibrium conformations: Schematic illustration of a test chain (shown in red) adopting different representative nonequilibrium conformations: (a) polymers, with local stretching along the direction of pulling force, resembling stems and flowers,[63] (b) completely stretched chains in the shish of shish-kebab structures,[29,31,32,58] (c) knots,[64] and (d) polymer films with strong adsorption near the surface.[41]

DOI: 10.1021/acs.macromol.9b01195
Macromolecules XXXX, XXX, XXX−XXX

chains out of equilibrium, hints toward the possibility that general concepts may exist for predicting processing-induced nonequilibrium behavior of polymers.

PERSPECTIVES AND OUTLOOK

For a quantitative understanding of preparation-induced material properties, we need to consider the ever-changing structures and properties of nonequilibrated polymers on all relevant length and time scales. Such considerations could take advantage of the novel experiments[65−68] and sophisticated simulation techniques that have recently been reviewed by Gartner and Jayaraman.[69] For instance, in Figure 4 we have shown different representative nonequilibrium conformations and key parameters that might help modeling the nonequilibrium structure developed. One goal may be to derive quantitative structure−processing relations that account for path- and time-dependent properties of polymers during processing. As demonstrated earlier, any processing-induced deviations in molecular conformations defined for example via deviations from a Gaussian distribution of chain conformations may induce transient order. Such order arises from temporal correlations between monomers or polymer segments, potentially reflected in variable static and dynamic heterogeneities. Therefore, a comprehensive understanding of such volatile molecular correlations and heterogeneities may shed light on the mechanisms underlying the processing induced deviations in polymer properties. As highlighted by the three chosen examples, we hypothesize that an appropriate metric of such correlations could serve as a possible order parameter characterizing the behavior of polymers induced through processing. The three examples focused on one-component polymer solutions and melts where nonequilibrium chain conformations and intermolecular packing immediately dictate system properties. These nonequilibrium molecular aspects, however, also impact collective structure formation in more complex polymer systems. For instance, (i) the as-cast structure of glassy copolymer films features frozen-in composition fluctuations that may impact microphase separation after heating above the glass transition temperature, (ii) the highly stretched chain conformations during roll casting[70−73] dictate the final orientation of the copolymer morphology, and (iii) shear flow has been successfully employed to direct the orientation of self-assembled structures.[74−76] Additionally, these multicomponent systems feature nonequilibrium structures, such as, for example, defects in directed self-assembly that arise from processing (i.e., the kinetics of structure formation) but that are not directly related to nonequilibrium chain conformations.[77]

To explore and identify the presence of order parameters, we believe it is important to address the following fundamental questions: Under which conditions (for example, the extent of local vs global stretching, local order vs long-range orientation, and spatial and temporal fluctuations in the degree of entanglements) can we create the transient order? How can we bridge from such transient and variable molecular correlations to concepts based on entropic or enthalpic interactions established for equilibrium systems? Can we borrow ideas on heterogeneities and correlations from the complex dynamics[78−83] experienced by various materials on approaching dynamical arrest? Can local correlations of monomers propagate through chain connectivity and induce long-ranged interactions between topological constraints? In the following, we propose various simulations and experiments that may allow addressing these questions.

Experiments indicate that the time allowed for equilibration during sample preparation, such as the evaporation time in the fabrication of polymer films[16,17] or the adsorption time in the case of further annealing,[21,22] is an important control parameter characterizing the deviations in the resultant properties of polymer films. This time parameter may be a good starting point for simulations.[84,85] Simulations that mimic experimental conditions (e.g., spinning rate and solvent evaporation rate) can provide unique molecular-level insight into the variations in chain conformations and entanglement density of systems such as freshly coated films or stretched polymer fibers. However, in comparison with experiments, simulated systems are often much smaller and the accessible time scales are typically much shorter. Therefore, it would already be a great success if one could obtain a qualitative agreement for some features, for example, changes of the thickness[23,27] and different material properties as viscosity and glass transition temperature upon annealing.[21,22,41] Apart from reproducing experimental results, simulations may also identify new experimentally testable regimes. Molecular conformations can be directly, and continuously, monitored in simulations, and their contribution to the (local) stress field (defined via a virial expression) can be determined. With such simulations, it might be possible to understand the origin of residual stresses and the length and time scales over which effects related to metastable states persist. Furthermore, simulations may shed light on the length scales and the extent of spatial heterogeneities in the mechanical properties of such nonequilibrated polymer films.[86−88] On the other hand, recent advances[68] in the current state of the art of neutron scattering experiments (and data analysis) show promises to track the relaxation pathways as expressed through changes in polymer conformations on approaching equilibrium.

A powerful solving strategy to understand how nonequilibrium local structures affect macroscopic properties could come from experiments and simulations aiming at a rational understanding of nonequilibrium conformations resulting from polymer adsorption to a substrate. Equilibration of thin films prepared by spin coating seems to be driven by density fluctuations of monomers near the adsorbing interface.[47] As a starting point, we may utilize concepts developed through a simple analytical model[89] which highlights the importance of entropic (free energy) frustration and its thermodynamic consequences on the adsorption of a single chain. This model shows that if a polymer is adsorbed initially with a wrong sequence (e.g., a high-energy state), then any effort to minimize energy requires trajectories departing further away from the equilibrium state. Such topologically quenched states could kinetically freeze polymers almost indefinitely out of equilibrium. Using similar ideas for many interacting polymers in a crowded environment, as in the adsorption of polymer melts, we may anticipate a stronger topological frustration, a more complex free energy landscape, and much larger length scales of cooperative motion. Hence, minimizing the free energy at the adsorbing interface might require concerted rearrangements of several molecules. Furthermore, we could consider experiments where adsorption is driven over specific sites (e.g., on patterned surfaces), which would allow controlling nonequilibrium interfacial conformations. We would then explore how macroscopic quantities are affected by the adsorbed chains. In both cases, density variations of the

DOI: 10.1021/acs.macromol.9b01195
Macromolecules XXXX, XXX, XXX−XXX

adsorbed chains (or segments)—a collective quantity characterizing the configuration of the system—could serve as an order parameter for the process of adsorption.

To understand the heterogeneous character of nonequilibrated polymers, experiments (e.g., nonlinear dielectric spectroscopy[90]) and simulations could focus on higher-order nonlinear susceptibilities. These quantities, as already verified in the case of small molecules,[91,92] provide signatures of the nature and the length scale of dynamic heterogeneities. Extending the investigation to star-shaped polymers or other nonlinear architectures of polymers is highly recommended as these systems are inherently heterogeneous in terms of both density and dynamics.[93−96] Notably, recent experiments[26,93,96] show that glassy star-shaped polymers age at a significantly lower rate than the corresponding linear chains, suggesting the importance of macromolecular architecture for tuning the lifetime of the processing-induced deviations in conformations. Finally, we might gain information on processing-induced nonequilibrium states by considering analogies with supercooled liquids, i.e., the precursors of glasses, which are arguably the most widely studied nonequilibrium materials. As is well-established from simulations of bulk glass formers, the rapid increase in the relaxation time of liquids approaching the glass transition temperature may be associated with the appearance of so-called locally preferred structures,[78−83] quantifying a form of growing structural order within an amorphous material. Here, we may ask whether the experimentally observed long relaxation times of processing-induced nonequilibrium conformations of polymers are also accompanied by a growing degree of locally preferred structural motifs. Given a proper and unique definition, this "transient order" could serve as a reliable order parameter of nonequilibrium conformations.

To summarize, processing-induced nonequilibrium conformations, and the thereby created correlations between variable number of polymer segments, provide access to novel structural, dynamical, and mechanical properties. To design polymers or polymeric structures with desired and tunable properties requires a quantitative understanding of how properties of polymers depend on nonequilibrium conformations. Through the presented examples, we highlight common scientific challenges for apparently different scenarios, hinting at possibilities for developing quantitative concepts relating processing protocols to molecular conformations and to resultant properties. We have identified some possible future directions of research that will bring us toward realizing our goal of "molecular process design" by achieving quantitative processing−property relations based on a fundamental understanding of polymers in nonequilibrium conditions. Clearly, a concerted effort between theory, simulations, and experiments is required to identify suitable order parameters characterizing the preparation-induced nonequilibrium states in polymers. A better understanding of polymers in nonequilibrium conditions not only will introduce new research directions in fundamental materials science but also will establish how the choice of the processing protocol can act as an important and tunable control parameter in materials design. Ultimately, the ability to open up new processing-based pathways will enable a much broader spectrum of structural, dynamical, and mechanical properties that are unattainable in thermodynamic equilibrium, thus potentially creating a wealth of novel applications.

AUTHOR INFORMATION

Corresponding Authors

*E-mail: sivasurender.c@gmail.com.
*E-mail: snapolit@ulb.ac.be.
*E-mail: guenter.reiter@physik.uni-freiburg.de.

ORCID

Sivasurender Chandran: 0000-0003-0547-0282
Daniele Cangialosi: 0000-0002-5782-7725
Emmanouil Glynos: 0000-0002-0623-8402
Marcus Müller: 0000-0002-7472-973X
Murugappan Muthukumar: 0000-0001-7872-4883
Ullrich Steiner: 0000-0001-5936-339X
Jun Xu: 0000-0003-2345-0541
Simone Napolitano: 0000-0001-7662-9858
Günter Reiter: 0000-0003-4578-8316

Notes

The authors declare no competing financial interest.

Biographies

Sivasurender Chandran is currently a Research Project Leader at the Institute of Physics, University of Freiburg, Germany. Siva earned his M.Sc. (2008) in Materials Science at the Anna University, Chennai, and Ph.D. (2014) in Soft Condensed Matter Physics working with Prof. Jaydeep K Basu at the Indian Institute of Science (IISc), Bengaluru. Before becoming a Research Project Leader in 2017, he was a postdoctoral researcher in the group of Günter Reiter (2014−2016). His research focuses on understanding and controlling various nonequilibrium phenomena—glass transition, crystallization, aging, rheology, and wetting/dewetting—observed in polymers and colloids.

Jörg Baschnagel received his Habilitation in physics in 1999 from the University of Mainz (Germany) and was appointed Professor in the same year at the University of Strasbourg (France), where he has stayed ever since. He is heading the Theory and Simulation group at

DOI: 10.1021/acs.macromol.9b01195
Macromolecules XXXX, XXX, XXX−XXX

the Institut Charles Sadron in Strasbourg. His research interest is the physics of polymers, currently in particular the dynamics of polymers, polymer glass transition, and the properties of thin polymer films.

Daniele Cangialosi obtained his PhD in 2001 at the University of Palermo. From 2001 and 2004 he was in The Netherlands, Technical University of Delft, for a 3 year postdoctoral fellowship. Before obtaining his current position, he was a postdoctoral fellow at the Donostia International Physics Center (DIPC) and at the Material Physics Center in San Sebastián (Spain). Since 2009, he is a Tenured Scientist at the Material Physics Center (Joint Center of the UPV/EHU and CSIC). His specialization is in dielectric relaxation spectroscopy and calorimetric techniques. The focus of his recent research activity is the problem of the glass transition in the bulk and under nanoscale confinement. He devoted special attention to the nonequilibrium dynamics, that is, the recovery of equilibrium in the so-called physical aging regime.

Koji Fukao was born in Osaka, Japan, and studied physics at Kyoto University. After receiving his Ph.D. in physics at Kyoto University and working at Kyushu University and Kyoto University as assistant Professor, he became associate Professor at Kyoto Institute of Technology in 2001. From 1992 to 1994, he stayed at Gert Strobls group at Freiburg University as an Alexander von Humboldt research fellow. Since 2007, he has been a full Professor of Physics at Ritsumeikan University in Shiga, Japan, to chair soft matter physics laboratory. Dr. Fukao has been an experimental physicist using scattering methods such as X-ray, light, neutron scattering, and dynamical methods such as dielectric relaxation spectroscopy and viscoelastic measurements. His primary research interest includes phase transition and dynamics in chain molecules, structure formation of polymers from the glassy state, the glass transition and dynamics in thin polymer films, and charge carrier motions in ionic liquid crystals.

Emmanouil Glynos studied physics at the University of Patras, and he received his PhD in 2007 in polymer physics at the University of Edinburgh. Until 2012, he was a postdoctoral research associate at the Department of Material Science and Engineering at the University of Michigan, working on the effect of macromolecular architecture on the physical properties of polymers at surfaces and interfaces. He was subsequently appointed as a Research Investigator at the University of Michigan at the Center for Solar and Thermal Energy Conversion where his research focused in addressing important scientific challenges associated with the structure−property relations and correlations of the morphology of the device active layer on the nanometer scale to the electrical and optical properties, the charge photogeneration, and overall performance of these systems. Since 2015 he is a Research Scientist at FORTH/IESL where the objective of his current research is to develop a fundamental understanding of, and controlling via macromolecular engineering, the structure and properties of nanostructured polymer materials that can be used as solid electrolytes in lithium−metal batteries and electrochromic devices and as active layers in organic photovoltaics.

Liesbeth M. C. Janssen is Assistant Professor in the department of Applied Physics at Eindhoven University of Technology, The Netherlands. She studied Chemistry at Radboud University Nijmegen and obtained her PhD in Theoretical Chemistry from the same university in 2012. Following postdoctoral stays at Columbia University, New York, working with Prof. David Reichman, and Heinrich-Heine University Düsseldorf, working with Prof. Hartmut Löwen, she established her own group in Eindhoven in 2017. Her research focuses on theory and simulation of nonequilibrium soft matter, including glass-forming materials and polymers, active matter, and glassy biological systems. In 2016, she was the recipient of the Mildred Dresselhaus Award and Guest Professorship at CUI, Hamburg. Her research has been supported by several personal

DOI: 10.1021/acs.macromol.9b01195
Macromolecules XXXX, XXX, XXX−XXX

fellowships, including an NWO Rubicon fellowship, Alexander von Humboldt research fellowship, and NWO START-UP grant.

Marcus Müller is Professor of Theoretical Physics at the Georg-August University, Göttingen, Germany. In 1995 he received his Ph.D. from the Johannes-Gutenberg-Universität, Mainz, Germany, working with Kurt Binder. After a TRACS visit at the EPCC Edinburgh, working with Mike Cates, and a Feodor Lynen fellowship with Michael Schick at the University of Washington, he returned back to Mainz and obtained his Habilitation in theoretical physics in 1999. Before joining the Georg-August University in 2005, he was an associate professor in the department of physics at the University of Wisconsin—Madison and a Heisenberg fellow of the German Science Foundation (DFG). The APS awarded him the 2004 John H. Dillon Medal, and in the same year, he received a Lichtenberg professorship from the Volkswagen foundation. He was elected APS fellow and is an Associate Editor of *ACS Macro Letters*. His research interests focus on computational, soft, and biological matter. Using computer simulations and self-consistent field calculations of coarse-grained models, he investigates the thermodynamics and kinetics of collective ordering processes of polymer blends, the directed self-assembly of copolymer materials, and processes that alter the topology of biological membranes.

Murugappan Muthukumar is the Wilmer D. Barrett Distinguished Professor of Polymer Science and Engineering at the University of Massachusetts, Amherst, where he has been a faculty member since 1983. Muthu earned his B.Sc. (1970) and M. Sc. (1972) degrees in Chemistry from University of Madras, India, and a Ph.D. (1979) in Chemical Physics working with Karl Freed at the University of Chicago. After working with Sir Sam Edwards of the Cavendish Laboratory, University of Cambridge, UK, he was a faculty member at the Illinois Institute of Technology from 1981 to 1983. He has received several awards from the American Physical Society and the American Chemical Society. His research interests include fundamental aspects of physics of charged macromolecules, polymer crystallization, virus assembly, and macromolecular basis of human vision.

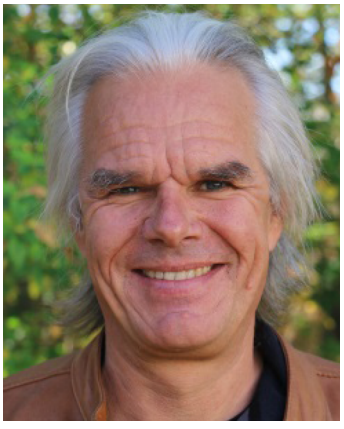

Ullrich (Ulli) Steiner studied physics at the University of Konstanz, Germany. He gained his Ph.D. in 1993, working with Prof. J. Klein and Prof. G. Schatz at the Weizmann Institute, Israel. After postdoc positions at the Weizmann Institute and the Institute Charles Sadron, France, he returned to Konstanz where he finished his Habilitation in 1998. He joined the faculty of the University of Groningen as full professor in 1999 and became the John Humphrey Plummer Professor of Physics of Materials at the University of Cambridge in 2004. Since 2014, he holds the chair of Soft Matter Physics at the Adolphe Merkle Institute in Switzerland.

Jun Xu is now an associate professor in Department of Chemical Engineering, Tsinghua University. He obtained his B.Sc. and Ph.D. degree at the Department of Chemical Engineering, Tsinghua University in 1997 and 2002, respectively. He was awarded the Alexander von Humboldt Research Fellowship for Experienced Researchers in 2011 and Feng Xingde Polymer Prize for winning "The Best Paper Nomination from China" published in the journal of Polymer in 2011. He was supported by the Program for New Century Excellent Talents in University in 2012. His research interests are in the field of polymer crystallization, biodegradable polymers, bioinspired materials, self-healing and recyclable polymers, 3-D printing, and so on. His work has revealed the twisting process of lamellar crystals in the polymer banded spherulites and what directs the twisting sense. He is now focusing on the nucleation mechanism of polymer lamellar crystals via combining theory and experiments.

DOI: 10.1021/acs.macromol.9b01195
Macromolecules XXXX, XXX, XXX−XXX

Simone Napolitano studied Materials Science at the Università di Pisa and received his PhD in Polymer Physics from KULeuven in 2008 and went on to complete postdoctoral work at the Research Foundation Flanders (FWO). In 2011, he joined the Université libre de Bruxelles (ULB). There he serves the Faculty of Science as associate professor and leads the Laboratory of Polymers and Soft Matter Dynamics and the group of Experimental Soft Matter and Thermal Physics. His research focuses on the molecular origin of the glass transition and the correlation between structure and dynamics in polymers and small molecules under nanoscopic confinement. His group is currently working on the physics of irreversible adsorption and on nonequilibrium phenomena in confined soft matter.

Günter Reiter has been a professor of experimental polymer physics at the University of Freiburg, Germany, since 2008. He studied physics in Graz, Austria (PhD in 1987). After postdoctoral stays at the MPI for Polymer Research in Mainz, Germany, and the University of Illinois in Urbana−Champaign, USA, he was a researcher at the CNRS in Mulhouse, France. His research interests focus on the behavior and properties of polymers at interfaces, ordering and crystallization processes in complex systems, and the formation of functional structures on surfaces. He has been a Divisional Associate Editor for *PRL* and is serving as an Editor for *EPJ ST*.

■ ACKNOWLEDGMENTS

This work is an outcome of stimulating and intensive discussions among the authors, searching for a unifying approach to understand a wide spectrum of largely unexpected, variable, and novel properties of polymers. We acknowledge the funding support from the International Research Training Group (IRTG-1642) - Soft Matter Science, funded by the Deutsche Forschunggemeinschaft (DFG). S.C. acknowledges funding support from DFG via CH 1741/2-1. U.S. acknowledges partial funding from the Adolphe Merkle Foundation.

■ REFERENCES

(1) Geyer, R.; Jambeck, J. R.; Law, K. L. Production, Use, and Fate of all Plastics Ever Made. *Science advances* **2017**, *3*, No. e1700782.
(2) Mutha, N. H.; Patel, M.; Premnath, V. Plastics Materials Flow Analysis for India. *Resources, Conservation and Recycling* **2006**, *47*, 222−244.
(3) Tadmor, Z.; Gogos, C. G. *Principles of Polymer Processing*; John Wiley & Sons: 2013.
(4) Park, J. H.; Rutledge, G. C. 50th Anniversary Perspective: Advanced Polymer Fibers: High Performance and Ultrafine. *Macromolecules* **2017**, *50*, 5627−5642.
(5) Bates, C. M.; Bates, F. S. 50th Anniversary Perspective: Block Polymers − Pure Potential. *Macromolecules* **2017**, *50*, 3−22.
(6) Reiter, G. In *Non-equilibrium Phenomena in Confined Soft Matter: Irreversible Adsorption, Physical Aging and Glass Transition at the Nanoscale*; Napolitano, S., Ed.; Springer International Publishing: Cham, 2015; pp 3−23.
(7) Abetz, V.; Kremer, K.; Müller, M.; Reiter, G. Functional Macromolecular Systems: Kinetic Pathways to Obtain Tailored Structures. *Macromol. Chem. Phys.* **2019**, *220*, 1800334.
(8) Reiter, G.; Hamieh, M.; Damman, P.; Sclavons, S.; Gabriele, S.; Vilmin, T.; Raphaël, E. Residual Stresses in Thin Polymer Films cause Rupture and Dominate Early Stages of Dewetting. *Nat. Mater.* **2005**, *4*, 754.
(9) Barbero, D. R.; Steiner, U. Nonequilibrium Polymer Rheology in Spin-Cast Films. *Phys. Rev. Lett.* **2009**, *102*, 248303.
(10) Thomas, K. R.; Chenneviere, A.; Reiter, G.; Steiner, U. Nonequilibrium Behavior of Thin Polymer Films. *Phys. Rev. E* **2011**, *83*, 021804.
(11) Thomas, K. R.; Steiner, U. Direct Stress Measurements in Thin Polymer Films. *Soft Matter* **2011**, *7*, 7839−7842.
(12) Chowdhury, M.; Freyberg, P.; Ziebert, F.; Yang, A. C.-M.; Steiner, U.; Reiter, G. Segmental Relaxations have Macroscopic Consequences in Glassy Polymer Films. *Phys. Rev. Lett.* **2012**, *109*, 136102.
(13) Teng, C.; Gao, Y.; Wang, X.; Jiang, W.; Zhang, C.; Wang, R.; Zhou, D.; Xue, G. Reentanglement Kinetics of Freeze-Dried Polymers above the Glass Transition Temperature. *Macromolecules* **2012**, *45*, 6648−6651.
(14) Sheng, X.; Wintzenrieth, F.; Thomas, K. R.; Steiner, U. Intrinsic Viscoelasticity in Thin High-molecular-weight Polymer Films. *Phys. Rev. E* **2014**, *89*, 062604.
(15) Chandran, S.; Reiter, G. Transient Cooperative Processes in Dewetting Polymer Melts. *Phys. Rev. Lett.* **2016**, *116*, 088301.
(16) Chandran, S.; Handa, R.; Kchaou, M.; Al Akhrass, S.; Semenov, A. N.; Reiter, G. Time Allowed for Equilibration Quantifies the Preparation Induced Nonequilibrium Behavior of Polymer Films. *ACS Macro Lett.* **2017**, *6*, 1296−1300.
(17) Kchaou, M.; Alcouffe, P.; Chandran, S.; Cassagnau, P.; Reiter, G.; Al Akhrass, S. Tuning Relaxation Dynamics and Mechanical Properties of Polymer Films of Identical Thickness. *Phys. Rev. E: Stat. Phys., Plasmas, Fluids, Relat. Interdiscip. Top.* **2018**, *97*, 032507.
(18) Chandran, S.; Reiter, G. Segmental Rearrangements Relax Stresses in Nonequilibrated Polymer Films. *ACS Macro Lett.* **2019**, *8*, 646−650.
(19) Askar, S.; Evans, C. M.; Torkelson, J. M. Residual Stress Relaxation and Stiffness in Spin-coated Polymer Films: Characterization by Ellipsometry and Fluorescence. *Polymer* **2015**, *76*, 113−122.
(20) Cangialosi, D.; Boucher, V. M.; Alegría, A.; Colmenero, J. Physical Aging in Polymers and Polymer Nanocomposites: Recent Results and Open Questions. *Soft Matter* **2013**, *9*, 8619−8630.
(21) Napolitano, S.; Wübbenhorst, M. The Lifetime of the Deviations from Bulk Behaviour in Polymers Confined at the Nanoscale. *Nat. Commun.* **2011**, *2*, 260.
(22) Napolitano, S.; Capponi, S.; Vanroy, B. Glassy Dynamics of Soft matter under 1D Confinement: How Irreversible Adsorption affects Molecular packing, Mobility Gradients and Orientational

DOI: 10.1021/acs.macromol.9b01195
Macromolecules XXXX, XXX, XXX−XXX

Polarization in Thin Films. *Eur. Phys. J. E: Soft Matter Biol. Phys.* **2013**, *36*, 61.
(23) Miyazaki, T.; Nishida, K.; Kanaya, T. Contraction and Reexpansion of Polymer Thin Films. *Phys. Rev. E* **2004**, *69*, 022801.
(24) Kanaya, T.; Miyazaki, T.; Inoue, R.; Nishida, K. Thermal Expansion and Contraction of Polymer Thin Films. *Phys. Status Solidi B* **2005**, *242*, 595−606.
(25) Frieberg, B.; Glynos, E.; Green, P. F. Structural Relaxations of Thin Polymer Films. *Phys. Rev. Lett.* **2012**, *108*, 268304.
(26) Frieberg, B.; Glynos, E.; Sakellariou, G.; Green, P. F. Physical Aging of Star-shaped Macromolecules. *ACS Macro Lett.* **2012**, *1*, 636−640.
(27) Bhattacharya, M.; Sanyal, M. K.; Geue, T.; Pietsch, U. Glass Transition in Ultrathin Polymer Films: A Thermal Expansion Study. *Phys. Rev. E* **2005**, *71*, 041801.
(28) Kumaraswamy, G.; Issaian, A. M.; Kornfield, J. A. Shear-Enhanced Crystallization in Isotactic Polypropylene. 1. Correspondence between in Situ Rheo-Optics and ex Situ Structure Determination. *Macromolecules* **1999**, *32*, 7537−7547.
(29) Cui, K.; Ma, Z.; Tian, N.; Su, F.; Liu, D.; Li, L. Multiscale and Multistep Ordering of Flow-Induced Nucleation of Polymers. *Chem. Rev.* **2018**, *118*, 1840−1886.
(30) Su, F.; Zhou, W.; Li, X.; Ji, Y.; Cui, K.; Qi, Z.; Li, L. Flow-induced Precursors of Isotactic Polypropylene: An in Situ Time and Space Resolved Study with Synchrotron Radiation Scanning X-ray Microdiffraction. *Macromolecules* **2014**, *47*, 4408−4416.
(31) Azzurri, F.; Alfonso, G. C. Insights into Formation and Relaxation of Shear-induced Nucleation Precursors in Isotactic Polystyrene. *Macromolecules* **2008**, *41*, 1377−1383.
(32) Hamad, F. G.; Colby, R. H.; Milner, S. T. Lifetime of Flow-induced Precursors in Isotactic Polypropylene. *Macromolecules* **2015**, *48*, 7286−7299.
(33) Hamad, F. G.; Colby, R. H.; Milner, S. T. Transition in Crystal Morphology for Flow-induced Crystallization of Isotactic Polypropylene. *Macromolecules* **2016**, *49*, 5561−5575.
(34) Park, J. H.; Rutledge, G. C. Ultrafine High Performance Polyethylene Fibers. *J. Mater. Sci.* **2018**, *53*, 3049−3063.
(35) Shen, S.; Henry, A.; Tong, J.; Zheng, R.; Chen, G. Polyethylene Nanofibres with Very High Thermal Conductivities. *Nat. Nanotechnol.* **2010**, *5*, 251.
(36) Poudel, P.; Chandran, S.; Majumder, S.; Reiter, G. Controlling Polymer Crystallization Kinetics by Sample History. *Macromol. Chem. Phys.* **2018**, *219*, 1700315.
(37) De Gennes, P.-G. *Scaling Concepts in Polymer Physics*; Cornell University Press: 1979.
(38) Müller, M. In *Understanding Soft Condensed Matter via Modeling and Computation*; Shi, A.-C., Hu, W., Eds.; World Scientific: 2010; pp 47−83.
(39) Ediger, M. D.; Forrest, J. A. Dynamics Near Free Surfaces and the Glass Transition in Thin Polymer Films: A View to the Future. *Macromolecules* **2014**, *47*, 471−478.
(40) Alcoutlabi, M.; McKenna, G. B. Effects of Confinement on Material Behaviour at the Nanometre Size Scale. *J. Phys.: Condens. Matter* **2005**, *17*, R461.
(41) Napolitano, S.; Glynos, E.; Tito, N. B. Glass Transition of Polymers in Bulk, Confined Geometries, and Near Interfaces. *Rep. Prog. Phys.* **2017**, *80*, 036602.
(42) Hall, D. B.; Hooker, J. C.; Torkelson, J. M. Ultrathin Polymer Films Near the Glass Transition: Effect on the Distribution of α-relaxation Times as Measured by Second Harmonic Generation. *Macromolecules* **1997**, *30*, 667−669.
(43) Inoue, R.; Kanaya, T.; Nishida, K.; Tsukushi, I.; Taylor, J.; Levett, S.; Gabrys, B. Dynamic Anisotropy and Heterogeneity of Polystyrene Thin Films as Studied by Inelastic Neutron Scattering. *Eur. Phys. J. E: Soft Matter Biol. Phys.* **2007**, *24*, 55−60.
(44) Inoue, R.; Kanaya, T. *Glass Transition, Dynamics and Heterogeneity of Polymer Thin Films*; Springer: 2012; pp 107−140.
(45) Fukao, K.; Terasawa, T.; Nakamura, K.; Tahara, D. *Glass Transition, Dynamics and Heterogeneity of Polymer Thin Films*; Springer: 2012; pp 65−106.
(46) Perez-de Eulate, N. G.; Sferrazza, M.; Cangialosi, D.; Napolitano, S. Irreversible Adsorption Erases the Free Surface Effect on the T g of Supported Films of Poly (4-tert-butylstyrene). *ACS Macro Lett.* **2017**, *6*, 354−358.
(47) Panagopoulou, A.; Napolitano, S. Irreversible Adsorption Governs the Equilibration of Thin Polymer Films. *Phys. Rev. Lett.* **2017**, *119*, 097801.
(48) Napolitano, S.; Rotella, C.; Wuebbenhorst, M. Can Thickness and Interfacial Interactions Univocally Determine the Behavior of Polymers Confined at the Nanoscale. *ACS Macro Lett.* **2012**, *1*, 1189−1193.
(49) Schaller, R.; Feldman, K.; Smith, P.; Tervoort, T. A. High-performance Polyethylene Fibers Al dente: Improved Gel-spinning of Ultrahigh Molecular Weight Polyethylene using Vegetable Oils. *Macromolecules* **2015**, *48*, 8877−8884.
(50) Ren, L.; Ozisik, R.; Kotha, S. P.; Underhill, P. T. Highly Efficient Fabrication of Polymer Nanofiber Assembly by Centrifugal Jet Spinning: Process and Characterization. *Macromolecules* **2015**, *48*, 2593−2602.
(51) Greenfeld, I.; Sui, X.; Wagner, H. D. Stiffness, Strength, and Toughness of Electrospun Nanofibers: Effect of Flow-induced Molecular Orientation. *Macromolecules* **2016**, *49*, 6518−6530.
(52) Ward, I. M. *Structure and Properties of Oriented Polymers*; Springer Science & Business Media: 2012.
(53) Tripathi, A.; Whittingstall, P.; McKinley, G. H. Using Filament Stretching Rheometry to Predict Strand Formation and Processability in Adhesives and other Non-Newtonian Fluids. Rheol. *Rheol. Acta* **2000**, *39*, 321−337.
(54) Zhang, W.; Larson, R. G. A Metastable Nematic Precursor Accelerates Polyethylene Oligomer Crystallization as Determined by Atomistic Simulations and Self-consistent Field Theory. *J. Chem. Phys.* **2019**, *150*, 244903.
(55) Gee, R. G.; Lacevic, N.; Fried, L. E. Atomistic Simulations of Spinodal Phase Separation Preceding Polymer Crystallization. *Nat. Mater.* **2006**, *5*, 39−43.
(56) Anwar, M.; Berryman, J. T.; Schilling, T. Crystal Nucleation Mechanism in Melts of Short Polymer Chains under Quiescent Conditions and under Shear Flow. *J. Chem. Phys.* **2014**, *141*, 124910.
(57) Stepanow, S. Kinetic Mechanism of Chain Folding in Polymer Crystallization. *Phys. Rev. E* **2014**, *90*, 032601.
(58) Hamad, F. G.; Colby, R. H.; Milner, S. T. Onset of Flow-induced Crystallization Kinetics of Highly Isotactic Polypropylene. *Macromolecules* **2015**, *48*, 3725−3738.
(59) Doufas, A. K.; Dairanieh, I. S.; McHugh, A. A Continuum Model for Flow-induced Crystallization of Polymer Melts. *J. Rheol.* **1999**, *43*, 85−109.
(60) Doufas, A. K.; McHugh, A.; Miller, C. Simulation of Melt Spinning Including Flow-induced Crystallization: Part I. Model Development and Predictions. *J. Non-Newtonian Fluid Mech.* **2000**, *92*, 27−66.
(61) Custodio, F. J. M. F.; Steenbakkers, R. J. A.; Anderson, P. D.; Peters, G. W. M.; Meijer, H. E. H. Model Development and Validation of Crystallization Behavior in Injection Molding Prototype Flows. *Macromol. Theory Simul.* **2009**, *18*, 469−494.
(62) Graham, R. S. Modelling Flow-induced Crystallisation in Polymers. *Chem. Commun.* **2014**, *50*, 3531−3545.
(63) Brochard-Wyart, F. Polymer Chains Under Strong Flows: Stems and Flowers. *Europhys. Lett.* **1995**, *30*, 387−392.
(64) de Gennes, P. G. Tight Knots. *Macromolecules* **1984**, *17*, 703−704.
(65) Sinha, S. K.; Jiang, Z.; Lurio, L. B. X-ray Photon Correlation Spectroscopy Studies of Surfaces and Thin Films. *Adv. Mater.* **2014**, *26*, 7764−7785.
(66) Grübel, G.; Stephenson, G. B.; Gutt, C.; Sinn, H.; Tschentscher, T. XPCS at the European X-ray Free Electron Laser Facility. *Nucl. Instrum. Methods Phys. Res., Sect. B* **2007**, *262*, 357−367.

DOI: 10.1021/acs.macromol.9b01195
Macromolecules XXXX, XXX, XXX−XXX

(67) Müller-Buschbaum, P. The Active Layer Morphology of Organic Solar Cells Probed with Grazing Incidence Scattering Techniques. *Adv. Mater.* **2014**, *26*, 7692−7709.
(68) Wang, Z.; Lam, C. N.; Chen, W.-R.; Wang, W.; Liu, J.; Liu, Y.; Porcar, L.; Stanley, C. B.; Zhao, Z.; Hong, K.; Wang, Y. Fingerprinting Molecular Relaxation in Deformed Polymers. *Phys. Rev. X* **2017**, *7*, 031003.
(69) Gartner, T. E., III; Jayaraman, A. Modeling and Simulations of Polymers: A Roadmap. *Macromolecules* **2019**, *52*, 755−786.
(70) Albalak, R. J.; Thomas, E. L. Roll-Casting of Block Copolymers and of Block Copolymer-Homopolymer Blends. *J. Polym. Sci., Part B: Polym. Phys.* **1994**, *32*, 341−350.
(71) Villar, M. A.; Rueda, D. R.; Ania, F.; Thomas, E. L. Study of Oriented Block Copolymers Films obtained by Roll-Casting. *Polymer* **2002**, *43*, 5139−5145.
(72) Xu, T.; Goldbach, J. T.; Russell, T. P. Sequential, Orthogonal Fields: A Path to Long-Range, 3-D Order in Block Copolymer Thin Films. *Macromolecules* **2003**, *36*, 7296−7300.
(73) Müller, M.; Tang, J. Alignment of Copolymer Morphology by Planar Step Elongation during Spinodal Self-Assembly. *Phys. Rev. Lett.* **2015**, *115*, 228301.
(74) Riise, B. L.; Fredrickson, G. H.; Larson, R. G.; Pearson, D. S. Rheology and Shear-Induced Alignment of Lamellar Diblock and Triblock Copolymers. *Macromolecules* **1995**, *28*, 7653−7659.
(75) Chen, Z.-R.; Kornfield, J. A. Flow-induced Alignment of Lamellar Block Copolymer Melts. *Polymer* **1998**, *39*, 4679−4699.
(76) Schneider, L.; Heck, M.; Wilhelm, M.; Müller, M. Transitions between Lamellar Orientations in Shear Flow. *Macromolecules* **2018**, *51*, 4642−4659.
(77) Li, W.; Müller, M. Defects in the Self-Assembly of Block Copolymers and Their Relevance for Directed Self-Assembly. *Annu. Rev. Chem. Biomol. Eng.* **2015**, *6*, 187−216.
(78) Frank, F. C. Supercooling of Liquids. *Proc. R. Soc. London A* **1952**, *215*, 43−46.
(79) Tarjus, G.; Kivelson, S. A.; Nussinov, Z.; Viot, P. The Frustration-based Approach of Supercooled Liquids and the Glass Transition: A Review and Critical Assessment. *J. Phys.: Condens. Matter* **2005**, *17*, R1143.
(80) Tanaka, H.; Kawasaki, T.; Shintani, H.; Watanabe, K. Critical-like Behaviour of Glass-forming Liquids. *Nat. Mater.* **2010**, *9*, 324.
(81) Kawasaki, T.; Tanaka, H. Structural Signature of Slow Dynamics and Dynamic Heterogeneity in Two-dimensional Colloidal Liquids: Glassy Structural Order. *J. Phys.: Condens. Matter* **2011**, *23*, 194121.
(82) Watanabe, K.; Kawasaki, T.; Tanaka, H. Structural Origin of Enhanced Slow Dynamics Near a Wall in Glass-forming Systems. *Nat. Mater.* **2011**, *10*, 512.
(83) Royall, C. P.; Williams, S. R. The Role of Local Structure in Dynamical Arrest. *Phys. Rep.* **2015**, *560*, 1−75.
(84) Peter, S.; Meyer, H.; Baschnagel, J. Molecular Dynamics Simulations of Concentrated Polymer Solutions in Thin Film Geometry. I. Equilibrium Properties Near the Glass Transition. *J. Chem. Phys.* **2009**, *131*, 014902.
(85) Peter, S.; Meyer, H.; Baschnagel, J. Molecular Dynamics Simulations of Concentrated Polymer Solutions in Thin Film Geometry. II. Solvent Evaporation Near the Glass Transition. *J. Chem. Phys.* **2009**, *131*, 014903.
(86) Yoshimoto, K.; Jain, T. S.; Workum, K. V.; Nealey, P. F.; de Pablo, J. Mechanical Heterogeneities in Model Polymer Glasses at Small Length Scales. *Phys. Rev. Lett.* **2004**, *93*, 175501.
(87) Mizuno, H.; Mossa, S.; Barrat, J.-L. Measuring Spatial Distribution of the Local Elastic Modulus in Glasses. *Phys. Rev. E* **2013**, *87*, 042306.
(88) Barrat, J.-L.; Baschnagel, J.; Lyulin, A. Molecular Dynamics Simulations of Glassy Polymers. *Soft Matter* **2010**, *6*, 3430−3446.
(89) Muthukumar, M. Chain Entropy: Spoiler or Benefactor in Pattern Recognition? *Proc. Natl. Acad. Sci. U. S. A.* **1999**, *96*, 11690−11692.
(90) Richert, R. *Nonlinear Dielectric Spectroscopy*; Springer International Publishing: 2018.
(91) Bauer, T.; Lunkenheimer, P.; Loidl, A. Cooperativity and the Freezing of Molecular Motion at the Glass Transition. *Phys. Rev. Lett.* **2013**, *111*, 225702.
(92) Albert, S.; Bauer, T.; Michl, M.; Biroli, G.; Bouchaud, J.-P.; Loidl, A.; Lunkenheimer, P.; Tourbot, R.; Wiertel-Gasquet, C.; Ladieu, F. Fifth-order Susceptibility Unveils Growth of Thermodynamic Amorphous Order in Glass-formers. *Science* **2016**, *352*, 1308−1311.
(93) Chremos, A.; Glynos, E.; Green, P. F. Structure and Dynamical Intra-molecular Heterogeneity of Star Polymer Melts above Glass Transition Temperature. *J. Chem. Phys.* **2015**, *142*, 044901.
(94) Srivastva, D.; Nikoubashman, A. Flow Behavior of Chain and Star Polymers and Their Mixtures. *Polymers* **2018**, *10*, 599.
(95) Ciarella, S.; Sciortino, F.; Ellenbroek, W. G. Dynamics of Vitrimers: Defects as a Highway to Stress Relaxation. *Phys. Rev. Lett.* **2018**, *121*, 058003.
(96) Frieberg, B. R.; Glynos, E.; Stathouraki, M.; Sakellariou, G.; Green, P. F. Glassy Dynamics of Polymers with Star-Shaped Topologies: Roles of Molecular Functionality, Arm Length, and Film Thickness. *Macromolecules* **2017**, *50*, 3719−3725.

DOI: 10.1021/acs.macromol.9b01195
Macromolecules XXXX, XXX, XXX−XXX

Macromolecules

Cite This: Macromolecules 2019, 52, 6935−6942

Article

pubs.acs.org/Macromolecules

Mesoscale Dynamics in Melts of Single-Chain Polymeric Nanoparticles

Arantxa Arbe,[*,†] Jon Rubio-Cervilla,[†,‡] Angel Alegría,[†,‡] Angel J. Moreno,[†,§] José A. Pomposo,[†,‡,∥] Beatriz Robles-Hernández,[§] Paula Malo de Molina,[§,▽] Peter Fouquet,[⊥] Fanni Juranyi,[#] and Juan Colmenero[†,‡,§]

[†]Centro de Física de Materiales (CFM) (CSIC-UPV/EHU)-Materials Physics Center (MPC), Paseo Manuel de Lardizabal 5, E-20018 San Sebastián, Spain

[‡]Departamento de Física de Materiales (UPV/EHU), Apartado 1072, 20080 San Sebastián, Spain

[§]Donostia International Physics Center (DIPC), Paseo Manuel de Lardizabal 4, E-20018 San Sebastián, Spain

[∥]IKERBASQUE-Basque Foundation for Science, María Díaz de Haro 3, 48013 Bilbao, Spain

[⊥]Institut Laue−Langevin, BP 156, 38042 Grenoble Cedex 9, France

[#]Laboratory for Neutron Scattering, Paul Scherrer Institut, CH-5232 Villigen, Switzerland

Supporting Information

ABSTRACT: Through a combination of neutron scattering, dielectric spectroscopy, and rheological measurements we study the impact of purely intramolecular cross-linking on a melt fully made of polymeric single-chain nanoparticles (SCNPs)—a novel class of ultrasoft nano-objects. While the α-relaxation is unaffected with respect to the reference melt of linear chains, the emerging polymer/colloid duality of SCNPs leads to the almost complete smearing out of the rubbery plateau. This is the opposite effect to the creation of a permanent 3D network by intermolecular bonds. In addition, neutron scattering shows that a new relaxation mechanism slower than the α-relaxation appears at intermediate length scales. These are beyond the interchain distance but yet far from the hydrodynamic regime. This new slow relaxation—also detected by dielectric spectroscopy—contributes to the hierarchy of processes needed for the full relaxation of the SCNP melt and is tentatively related to the heterogeneities provoked by the internal multiloop topology of the SCNPs and the segregation of their internal domains.

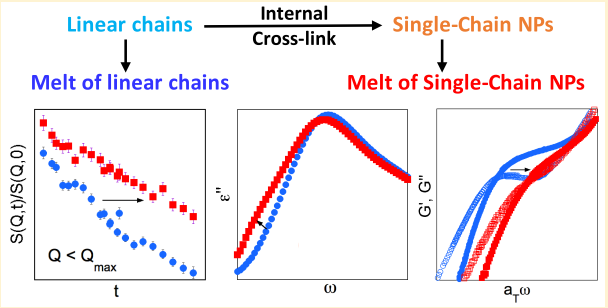

INTRODUCTION

The chance discovery of vulcanization by Goodyear in 1839 probably constituted the most revolutionary event in the history of polymer industry. In this process, creation of a relatively small amount of intermolecular cross-links between different macromolecules leads to a permanent 3-D network with an associated spectacular transformation of the macroscopic properties of the material above the glass transition, from a (peculiar) liquid to a rubber-like behavior. How does the system behave if cross-links are of purely *intramolecular* nature is an intriguing still unsolved question we are trying to answer in this work. To do that, we will consider a polymer melt only composed by so-called single-chain nanoparticles (SCNPs), which are obtained by intramolecular cross-linking of individual macromolecular chains. This system experimentally realizes the situation of a purely intramolecular cross-linked polymer bulk.

SCNPs are soft nano-objects halfway between linear chains and "standard" nanoparticles. Thanks to their ultrasmall size, softness, and internal compartmentalization they are believed to be a fundamental ingredient in the field of nanotechnology.[1−10] Due to their similarities with intrinsically disordered proteins (IDP)[11,12] —ubiquitous in living organisms—SCNPs can also be used as synthetic mimics, free of specific interactions, of relevant biomacromolecules to investigate problems as important as the influence of crowding in the cellular environment. In general, studies of systems based on SCNPs allow taking a look on the still scarcely explored interface between the soft matter fields of polymers and colloids.[13]

With these ideas in mind, in this work we made a concerted effort by combining advanced chemistry and a battery of different experimental tools, including "macroscopic" (calorimetry, dielectric, and mechanical spectroscopy) and "microscopic" (neutron diffraction and neutron spin echo, NSE) techniques to study the unique properties of a SCNPs melt.

Received: June 19, 2019
Revised: August 7, 2019
Published: September 5, 2019

DOI: 10.1021/acs.macromol.9b01264
Macromolecules 2019, 52, 6935−6942

We employed SCNPs based on tetrahydrofuran (THF). The choice of this system obeys its availability in deuterated version,[14] low glass transition temperature (T_g)—both facilitating the neutron investigation and allowing the application of different experimental techniques over a wide frequency/temperature range—and its chemical simplicity.

Neutron scattering techniques, providing spatial resolution through the scattering vector (Q) dependence of the measured magnitudes, have been applied to perdeuterated systems, to follow collective features. The comparison with a bulk sample composed by the long linear counterpart chains (precursor macromolecules without internal cross-links) demonstrates that the structure and dynamics at local length scales including the interchain distances (in particular, the structural relaxation) are hardly sensitive to intramolecular cross-links. We remind that, in general, this is also the behavior observed when the cross-links are of intermolecular nature (permanent 3D network). However, in our case, rheological experiments not only show the absence of a rubbery plateau—characteristic of a 3D network—but also a striking reduction of the transient rubber-like plateau, due to entanglements, observed in the melt of linear precursor chains. On the other hand, we were able to extend our neutron experiments to the until now almost virgin territory of the so-called intermediate length scales (ILS). The ILS region corresponds to length scales larger than the typical intermolecular (for small molecules) or interchain (for polymeric objects) distances but not yet in the hydrodynamic regime. At ILS we observe a pronounced slowdown of the collective dynamics, associated with emerging structural heterogeneities with a characteristic length of about 1 nm. Moreover, the dielectric relaxation spectra reveal an enhanced intensity in the frequency region below the α-relaxation loss peak.

The combination of the results from all of these techniques has been crucial to elaborate a consistent picture. We conclude that the local globulation and compartmentalization into domains composed by internal loops induced by the intramolecular cross-links[11,15,16] has three main impacts: (i) introducing heterogeneities with nanometer length scale; (ii) increasing the complexity of the dynamics; in particular, a new relevant relaxation mechanism appears, presumably associated with the internal domains; and (iii) strongly hampering the formation of entanglements among macromolecules.

EXPERIMENTAL DETAILS

Materials. Tetrahydrofuran (≥99.9%, Scharlab) and epichlorohydrin (99%, Aldrich) were dried over CaH_2, degassed, and distilled in a vacuum line prior to use. Tris(pentafluorophenyl)borane (95%, Aldrich) was sublimed at 60 °C in a coldfinger condenser. Tetrahydrofuran-d_8 (99.5 atom % D, Acros), epichlorohydrin-d_5 (≥98 atom % D, Aldrich), dichloromethane (reagent grade, Aldrich), *N*,*N*-dimethylformamide (≥99.8%, Scharlab), sodium azide (≥99.5%, Aldrich), and methanol (≥99.9%, Scharlab) were used as received.

Synthesis of Protonated and Deuterated Copolymers. All reactions were performed in bulk conditions under an argon atmosphere using Schlenk flasks. For the synthesis of the protonated copolymer (hCop), $B(C_6F_5)_3$ (20 mg, 0.04 mmol), tetrahydrofuran (2.50 mL, 30.8 mmol), and epichlorohydrin (0.63 mL, 8.1 mmol) were mixed in a 25 mL Schlenk flask and stirred at room temperature for 48 h. The resulting crude product was precipitated in cold methanol, yielding a sticky transparent copolymer (hCop: 1.75 g, 59% yield, M_w = 33.4 kg/mol, M_w/M_n = 1.13). The same procedure was followed for the synthesis of the deuterated sample. Hence, $B(C_6F_5)_3$ (72 mg, 0.14 mmol), tetrahydrofuran-d_8 (8.4 mL, 103 mmol), and epichlorohydrin-d_5 (1.8 mL, 23 mmol) were used to obtain the deuterated copolymer (dCop: 5.61 g, 53% yield, M_w = 36.8 kg/mol, M_w/M_n = 1.23).

Functionalization of the Protonated and Deuterated Copolymers To Obtain the Protonated and Deuterated Precursors. In a typical azidation procedure, 1.0 g of the protonated copolymer was dissolved in DMF (40 mL) in a round-bottom flask. NaN_3 (330 mg, 2 equiv) was added, and the mixture was left stirring for 24 h at 60 °C. The crude product was precipitated in a 1:1 H_2O/MeOH mixture and dried under reduced pressure and at 50 °C in a vacuum oven to yield the azide-containing protonated precursor (hPrec: 0.85 g, 85% yield). The same procedure was followed to obtain the deuterated precursor (dPrec: 0.82 g, 82% yield). According to the analysis of Raman scattering bands at around 750 cm^{-1}, corresponding to C−Cl vibrations, about 30% of the chlorine atoms of the copolymer were substituted by azide groups. These results were confirmed by means of elemental analysis.

Synthesis of SCNPs from the Protonated and Deuterated Precursors. Single-chain nanoparticles (SCNPs) were synthesized via intramolecular azide photodecomposition.[14] In a typical procedure, 100 mg of precursor (hPrec or dPrec) was dissolved in distilled THF (100 mL, 1 mg/mL) in a vial covered with aluminum foil and exposed to UV irradiation (λ = 300−400 nm) for 3 h at room temperature. The solvent was evaporated at reduced pressure, and the resulting product was redissolved with CH_2Cl_2 (~0.5 mL) and precipitated in cold methanol. SCNPs (hNP or dNP) were obtained as yellowish viscous liquids (ca. 90% yield in both cases). The final product contained about 50% of unreacted azide groups as determined by means of the analysis of the infrared absorption band at around 2100 cm^{-1}. When considering together the copolymer composition (20% mol epichlorohydrin), the substituted chlorine atoms, and the finally reacted azide groups it results that the obtained SCNPs have on average an intramolecular cross-link every 54 main-chain carbons. These results were confirmed by means of elemental analysis. The chemical formula of dPrec and the induced cross-link are shown in Scheme 1.

Relaxation Techniques. Differential scanning calorimetry (DSC) measurements were carried out on 5−10 mg of sample using a Q2000 TA Instrument. A liquid nitrogen cooling system (LCNS) was used with a 25 mL/min helium flow rate. Measurements were performed using hermetic aluminum pans. The glass transition temperatures were determined as the inflection point of the reversing heat-flow signal as recoded during cooling at 3 K/min from 373 to 173 K.

Scheme 1. MD Snapshot of a Typical SCNP in Solution[a]

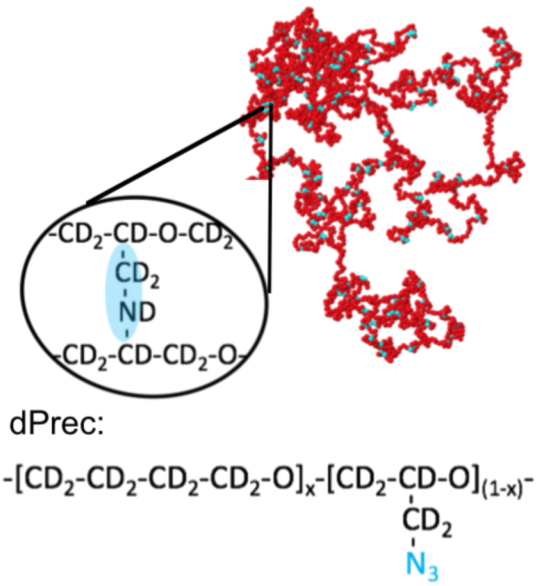

[a]Chemical formula of dPrec and a scheme of a cross-link in the real system are also shown.

DOI: 10.1021/acs.macromol.9b01264
Macromolecules 2019, 52, 6935−6942

Temperature-modulated experiments (MDSC) were performed using a sinusoidal variation of 0.5 K amplitude and 60 s period. The glass-transition temperatures (T_g), of 202 (hPrec) and 199 K (dPrec), increased about 1 K in the corresponding SCNPs' bulk. No signatures of crystallinity were found.

Broadband dielectric spectroscopy (BDS) experiments were conducted by using an Alpha dielectric analyzer (Novocontrol) and an E4991A RF-Impedance Analyzer (Agilent) to determine the complex dielectric permittivity ($\varepsilon^*(\omega) = \varepsilon'(\omega) - i\varepsilon(\omega)$) over the frequency range $f = (\omega/2\pi)$ from 10^{-2} to 10^8 Hz. Samples were placed between two flat gold-plated electrodes (10 or 20 mm diameter) forming a parallel plate capacitor with a 0.1 mm thick spacer of Teflon of negligible area between them. The temperature was controlled by a nitrogen-jet stream with a Novocontrol Quatro temperature controller. Frequency sweeps were performed at constant temperature with a stability better than 0.05 K.

Rheological experiments in the linear regime in the frequency range ≈ 0.03−16 Hz were performed by using an ARES torsional rheometer with a parallel plate geometry (8 mm diameter) with a typical gap distance of 0.5 mm.

Neutron Scattering. With the Neutron Spin Echo (NSE) spectrometer IN11C[17] at the Institute Laue Langevin (ILL) we studied the normalized dynamic structure factor $S(Q,t)/S(Q,0)$ on the deuterated samples. The scattered neutron intensity is then dominated by the coherent contribution, where all atomic pair correlations are approximatelly equally weighted.[18] The multidetector at IN11C covers an angular range of 30° in the horizontal plane. It was placed at 20°, 50°, and 80° scattering angle for its central detector. With an incident wavelength of 5.5 Å, a Q range of $0.15 \leq Q \leq 1.64$ Å^{-1} and a time range from 5 ps to 0.7 ns were explored. The experiments were performed at temperatures of 280, 320, and 360 K. To determine the resolution, a TiZi sample was used.

The structural properties were explored on the deuterated systems by small angle neutron scattering (SANS) at D11 at the ILL with an incident wavelength of 6.0 Å at 296 K. Samples were filled in quarz cuvettes (QS, Hellma) (sample thickness = 1 mm). This information was complemented at high Q values by the integrated intensity of spectra recorded by the time-of-flight FOCUS instrument[19] at the Paul Scherrer Institut.

RESULTS

The structure factor $S(Q)$—static limit of $S(Q,t)$—presents a well-defined amorphous halo centered at around Q_{max} = 1.4 Å^{-1} for both linear precursor and SCNPs melts (see Figure 1a). In main-chain polymers, this peak can usually be attributed to correlations between atoms belonging to nearest neighbor chains,[20] separated by an average interchain distance $d \approx 2\pi/Q_{max}$. The value $d \approx 4.5$ Å is not appreciably disturbed by internal cross-links. The structural relaxation leading to the decay of these correlations is also unaltered, as shown by its characteristic time in Figure 1b and directly from the comparison of the NSE results at this Q_{max} (squares in Figure 2). In strong constrast, the collective relaxation of SCNPs at small Q values below Q_{max}—corresponding to the above introduced ILS region—is dramatically slowed down. This is illustrated with the results for $Q \approx 0.4$ Å^{-1} shown in Figure 2. The NSE curves at different Q values were described by stretched exponentials

$$\frac{S(Q,t)}{S(Q,0)} \propto \exp\left[-\left(\frac{t}{\tau_w}\right)^{\beta}\right] \quad (1)$$

with values of the stretching exponent β of 0.43 (280 K), 0.47 (320 K), and 0.55 (360 K). The average characteristic times obtained as $\langle\tau\rangle = \Gamma(1/\beta)\tau_w/\beta$ are shown in Figure 1b. While in the high Q range (Q > 0.7 Å^{-1} approx.) nearly indistinguishable results can be seen for both systems, at lower Q values the collective times show an opposite behavior for SCNPs and linear chains: they tend to continuously increase toward larger length scales for the former, whereas they show an acceleration and a tendency to reach a plateau at low Q values for the latter.

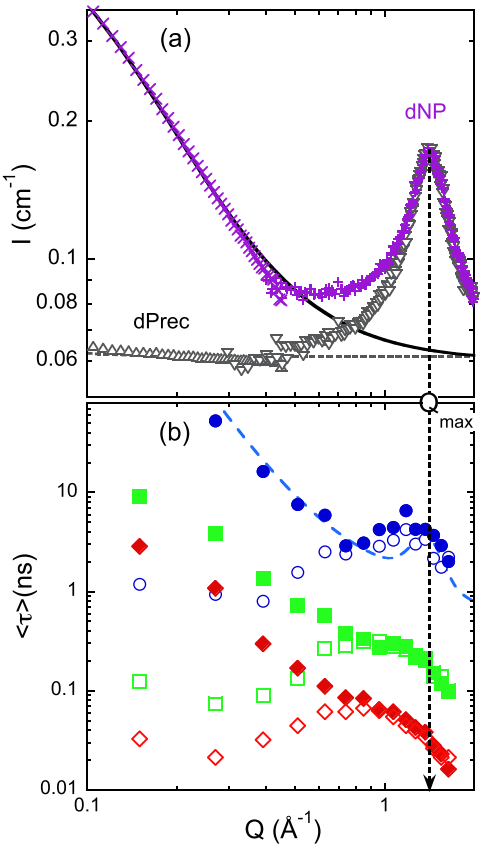

Figure 1. (a) Differential cross section of dPrec (up triangles, D11; down triangles, FOCUS) and dNP (crosses, D11; pluses, FOCUS). Dotted line marks its value for dPrec at ILS, and solid line includes an Ornstein−Zernike contribution. (b) Q dependence of the average collective characteristic times from NSE (empty symbols, dPrec; filled symbols, dNP) at 280 (circles), 320 (squares), and 360 K (diamonds). As an example, the dashed line shows the (anomalous) diffusive time for the 280 K data.[21]

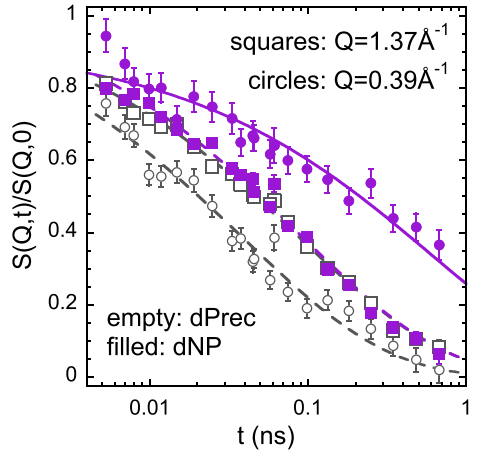

Figure 2. Normalized dynamic structure factor at $Q \approx Q_{max}$ and a representative Q value in the ILS region at 320 K. Lines are fits of eq 1 to dPrec (dashed lines) and dNP (solid lines) data with β = 0.47.

DOI: 10.1021/acs.macromol.9b01264
Macromolecules 2019, 52, 6935−6942

This leads to a strong decoupling of the time scales of the two systems that becomes more and more acute with decreasing Q, at least in the window accessed by the present experiments.

Though the investigations of collective dynamics of glass-forming systems at ILS are still very scarce, the available experimental results[22−24] and a recently proposed theoretical ansatz[25,26] point to a crossover at ILS from diffusion-dominated dynamics (high Q values, covering the first structure factor peak) toward a region at low Qs where the viscoelastic coupling of stress and density fluctuations dominates. Diffusive-like mechanisms predict a kind of maximum for the characteristic time in the neighborhood of Q_{max}—reminiscent of the deGennes narrowing[27]—together with a continuous slowing down with decreasing Q below the Q_{max} region. As an example, the dashed line in Figure 1b shows for T = 280 K the expected diffusive characteristic times deduced from incoherent scattering experiments on the protonated precursor[21] and applying a Sköld-like renormalization, $S_{coh}(Q, t) \approx S(Q)S_{inc}(Q/\sqrt{S(Q)}, t)$.[28] This slowing down becomes instead an acceleration in the crossover region at ILS,[25] and the collective times are expected to decrease toward the value experimentally accessed by macroscopic techniques in the $Q \rightarrow 0$ limit. Such a behavior is also qualitatively found in the present results on the linear precursor melt, as can be seen in Figure 1b. The crossover would occur in the region around $Q_c \approx 0.6$ Å^{-1}. Beyond a certain length scale—somehow related with Q_c—the system would appear as viscoelastically homogeneous. On the contrary, the behavior of the melt of SCNPs reminds a diffusion-dominated-like dynamics in the entire Q range covered, also well below Q_{max} (see the case of T = 280 K in Figure 1b). For this sample, the expected crossover to a nondiffusive characteristic time would thus be strongly shifted to low Q values (even below those accessed by the IN11C window), implying—within the proposed ansatz—that the SCNPs bulk would behave viscoelastically homogeneous only at extremely large length scales.

Structural heterogeneities responsible for such a dynamical behavior at ILS are evidenced by a pronounced increase of the low-Q scattering with respect to that in the precursor (see Figure 1a). Such an excess can be well accounted for by an Ornstein−Zernike expression,[29] $I_{OZ} \propto 1/[1 + (Q\xi)^2]$, with a value of ∼9 Å for the characteristic length ξ.

The dielectric spectroscopy (DS) results at approximately T_g + 20 K are shown in Figure 3. In this figure the contribution from the conductivity has been subtracted for both the precursor and the SCNP data (see full data in Figures S1 and S2 of the Supporting Information (SI)). Following the analysis explained in detail in the Appendix, the precursor data are decomposed in an α- and a β-process. These contributions can be seen as dashed−dotted lines in Figure 3. The permittivity loss peak characteristic times of the α- and β-processes in the precursor are represented in Figure 4. The DS α-relaxation times are longer than those observed by NSE at Q_{max}, suggesting large dipolar correlations in this sample. As can be appreciated in Figure 3, internal cross-linking produces a broadening of the main loss dielectric peak, mainly affecting its low-frequency flank, and a slight apparent shift of this maximum. Since the neutron study demonstrates that the properties at local and intermolecular length scales are practically insensitive to internal cross-linking, the functional forms and characteristic times of the dielectric β- and α-processes of the SCNPs can be fixed to those determined from the precursor study. However, to describe the DS results in this way we have to assume that the amplitude of the α-peak is smaller that in the SCNPs, i.e., that not all of the polarization relaxes through this process, but only a fraction x_a. Introducing the latter as a fit parameter (see Appendix), the relaxational contribution of the remaining fraction $1 - x_a$ was deduced. Figure 3 illustrates the decomposition obtained for an intermediate temperature. The additional process has a maximum at lower frequencies than the α-peak and is highly asymmetric. The temperature dependence of x_a and the shape parameter γ (see Appendix) of the low-frequency contribution are shown in Figure S3 of the SI. Except for temperatures close to T_g, the values of these parameters are independent of the temperature. From Figure S3 we conclude that the additional slow process found in the SCNPs accounts for the relaxation of

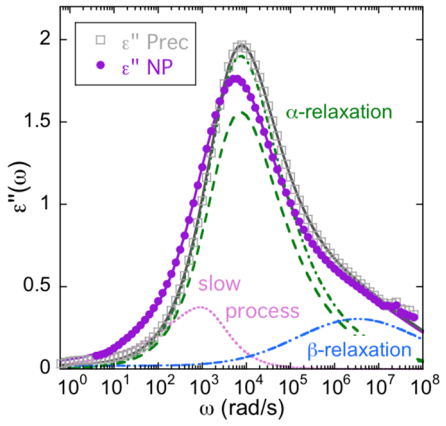

Figure 3. Dielectric losses at 220 K (conductivity subtracted). Solid lines are fitting curves considering a β-relaxation, an α-relaxation, and an additional slow contribution in the case of the SCNPs.

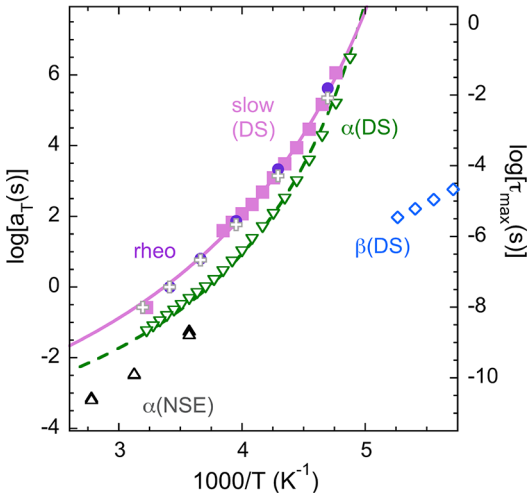

Figure 4. Relaxation map combining the rheological shift factors for precursors (empty crosses) and SCNPs (filled circles) and relaxation times (from the maxima of the imaginary part of the susceptibility function): squares, down triangles, and diamonds correspond to the slow DS, the α-process, and the β-process, respectively. Solid line shows the VFT fitting the temperature dependence of the rheological shift factors and the DS slow relaxations from the SCNPs melt. Dashed line is the VFT fit of the α-relaxation times. Up triangles show the NSE characteristic times at Q_{max} for precursor (empty) and SCNP (filled) melts.

DOI: 10.1021/acs.macromol.9b01264
Macromolecules 2019, 52, 6935−6942

about 15% of the polarization. The temperature dependence of the characteristic time of this process is included in Figure 4. As the α-relaxation, the slower process observed in the SCNPs melt shows non-Arrhenius behavior. In both cases the description of the temperature dependence was made using a Vogel–Fulcher–Tamman (VFT) equation,[30−32] which reads as

$$\tau(T) = \tau_\infty \exp\left[\frac{B}{T - T_0}\right] \quad (2)$$

We assumed the same value of the preexponential factor $\tau_\infty = 10^{-12}$ s for both relaxational processes. The resulting values obtained for the Vogel temperature, T_0, and the energetic term, B, were $T_0 = 161.4$ K, $B = 1125$ K for the α-relaxation and $T_0 = 143.3$ K, $B = 1615$ K for the slower relaxation.

Moving to the rheological experiments, the master curves obtained for the real and imaginary parts of the shear modulus of the melts are presented in Figure 5. Let us first focus on the

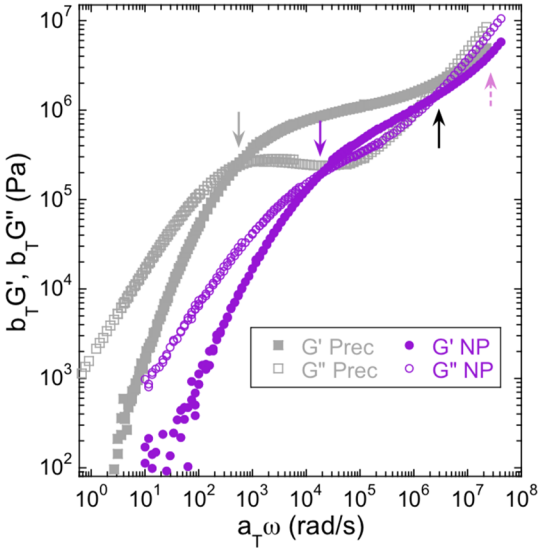

Figure 5. Rheological master curves (reference temperature 293 K). Arrows indicate the entanglement (up, solid), disentanglement (down, solid), and DS slow process (up, dotted) reduced frequencies.

linear precursor results. As it is typical for long linear chains,[29] these curves cross at two points: that at high frequencies reflects the onset of entanglement effects on the mechanical response, and that at low frequencies is the signature of the disentanglement of the chains. In linear polymers, the separation of these two points increases with the length of the macromolecules; in between, the reptation mechanism associated with the topological constraints imposed by neighboring chains ("entanglements") prevails, leading to a transient "soft-solid like" behavior of the melt. The impact of intramolecular cross-linking is striking. It produces a strong shift of the low-frequency crossing point to higher frequencies, such that the plateau in the shear modulus practically disappears in the melt of SCNPs. The transient rubber-like behavior smears out, and the system readily flows. The difference with respect to the *intermolecular* cross-linking impact on the rheological properties—persistent low-frequency plateaus reflecting the permanent 3D network structure[29]—is dramatic.

DISCUSSION

Our combined study shows that intrachain cross-linking does not change the local length scale properties (interchain average distance and dynamics of the α-relaxation) but has a strong impact at larger length scales. To provide a consistent picture of the experimental observations, we have to bear in mind that in the way SCNPs are synthesized (extremely diluted in a good solvent and with a relatively low fraction of reactive monomers in the precursors) their resulting morphology is rather sparse.[33−35] This is illustrated by the snapshot in Scheme 1. SCNPs contain internal loops and clusters of loops ("domains") of different sizes—but predominantly small—connected by flexible strands[11,12,15,36] and are highly penetrable. Interpenetration of them is indeed needed to fill the space and form a melt. Structurally, intrachain cross-links manifest in the heterogeneities—extra scattering length density fluctuations—with nanometric length scale. Close to cross-links and in particular within small domains, chain conformation and packing are expected to be different than in the rest of the bulk material. Internal bonds would impose an extra constraint for relaxation of the neighboring segments, provoking retardation of the decay of density fluctuations at ILS with respect to a melt of chemically identical chains with simple linear topology. Also, the internal domain topology itself could cause certain correlations to persist over time, rendering the crossover toward a viscoelastically homogeneous regime unaccessible in the explored NSE window. Determining the characteristic length at which the crossover to viscoelastic homogeneity is reached is a crucial issue that shall be addressed with new NSE experiments, pushing the low-Q limit of the study to lower Q values. How this length compares with the correlation length estimated for the heterogeneities of about 1 nm is an intriguing open question for this kind of system. Furthermore, the single chain dynamic structure factor of the SCNPs in bulk—accessible by NSE on a melt containing some labeled protonated SCNPs in a deuterated SCNPs matrix—is a key observable that will be addresed in future experiments to provide direct insight into the loopy internal—and center of mass—dynamics of these nano-objects in the melt.

The relaxation of the internal loops could also be at the origin of the slowly relaxing fraction of the polarization, explaining the additional "slow" dielectric process. An estimation of the size of the strands participating in this process delivers lengths on the order of the nanometer, coinciding with the heterogeneity size observed by neutron scattering. The estimation of this length scale, invoking as reference the chain statistics and dynamics of the linear chains,[29] is as follows. The precursor entanglement relaxation time obtained from rheology at 293 K is $\tau_e(293\ \mathrm{K}) = 2.45 \times 10^{-7}$ s. Moreover, τ_e is the relaxation time of the entanglement molecular weight M_e. This can be determined from the experimental plateau modulus $G_N = 1$ MPa, the polymer density $\rho = 1.1$ g/cm^3, the gas constant $R = 8.31$ J/mol K, and the temperature $T = 293$ K as $M_e = 4\rho RT/(5G_N) \approx 2000$ g/mol. Since for molecular masses below the entanglement molecular mass Rouse dynamics would apply ($\tau \approx M^2$), we can calculate the molecular weight of the chain strands involved in a mode with characteristic time equal to that of the slow dielectric process at this temperature, $\tau_{slow}(293\ \mathrm{K}) = 3.55 \times 10^{-8}$ s. This gives, through $\tau_{slow} = \tau_e M^2/M_e^2$, an involved mass of $M \approx 760$ g/mol. On the other hand, from SANS

DOI: 10.1021/acs.macromol.9b01264
Macromolecules 2019, 52, 6935−6942

experiments on a linear sample with 10% hPrec in 90% dPrec chains of M_w = 28 kg/mol we obtained a Gaussian form factor with average end-to-end distance R_{ee} = 125 Å (R_{ee}^2/M_w = 0.556 Å^2 mol/g). Taking this into account, a mass of $M \approx 760$ g/mol would correspond to an end-to-end chain strand distance of about 2 nm. Though of course this implicit mapping of the SCNP into the linear chain is a very crude approximation, it gives a rough estimation of the range of length scales involved in the slow DS process. We note that, in fact, the resulting value of 2 nm for the end-to-end chain strand distance (8 Å for the equivalent radius of gyration, assuming Gaussian statistics, $R_{ee}^2 = 6R_g^2$) is comparable with that deduced from the SANS experiments on the deuterated SCNPs melt (Ornstein–Zernike characteristic length of the heterogeneities).

In the rheological master curve the slow DS process is located close to the upper limit of the reduced frequency scale, i.e., prior to the onset of entanglements (see Figure 5). However, signatures of this process could be envisaged in the mechanical tan δ representation. The results obtained for tan $\delta = G''(\omega)/G'(\omega)$ for both precursor and SCNP bulks are shown in Figure 6. We note that the crossing points of the line tan δ = 1 mark the reduced frequencies corresponding to both the entanglement time (τ_e) and the disentanglement time (τ_d)[29] for both systems. The broadening of the low-frequency flank of the high-frequency peak is reminiscent of the experimental behavior observed by dielectric spectroscopy, giving rise to the slow DS process [τ_{slow}(293 K) = 3.55× 10^{-8} s, i.e., its characteristic frequency is 2.8 × 10^7 s^{-1}]. Then, at least qualitatively speaking, this broadening should be a mechanical signature of the dielectric slow DS process.

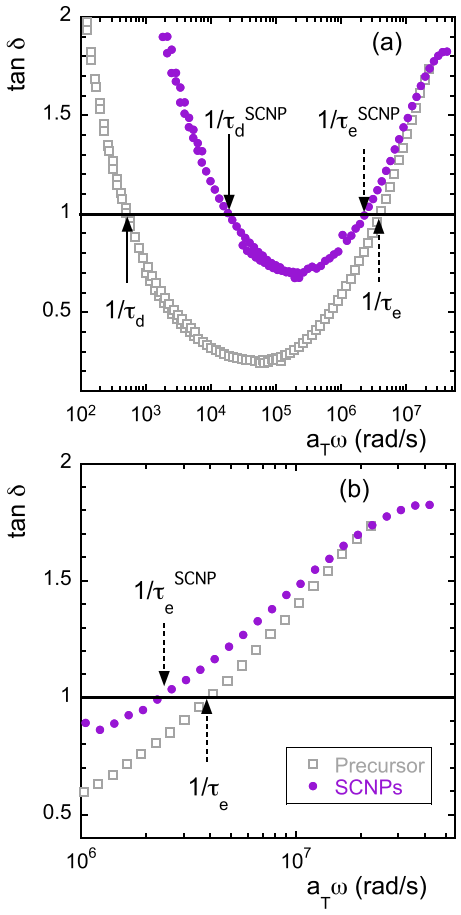

Figure 6. Reduced-frequency dependence of the tan $\delta = G''(\omega)/G'(\omega)$ corresponding to the rheological master curves shown in Figure 5 (empty squares, precursor; filled circles, SCNPs). (a) Results in a wide frequency range, while (b) blows up of the high-frequency region.

Accordingly, the temperature dependence of the dielectric slow process describes also well that of the shift factors used in the construction of the rheological master curves of the SCNPs (see Figure 4). This suggests that the relaxation of such newly appeared correlations associated with rigid "domains" is a prerequisite for the complete relaxation of the melt but is not directly responsible for the flow, since it takes place time decades before the disentanglement time (see Figure 5). Inspired by other architecturally complex polymer melts (stars, rings, ...), we may speculate that the flow would proceed in a highly hierarchical[37−39] and complex way (breaking of ultrasoft cages preceded by relaxations of branches and loops); in this case, it would probably be triggered by relaxation of the heterogeneities detected by SANS and reflected in the slow DS process, which seem to be related with the internal multiloop topology.

Particular discussion is deserved by the entanglements in the system. Blurring the chain contour has a strong impact on the ability of entanglement formation. The terminal relaxation with respect to the precursor bulk is clearly accelerated, showing an "effective" reduction of entanglements. This effect is by itself relevant and highly nontrivial since, unlike dense elastic spheres, our very weakly cross-linked SCNPs are strongly interpenetrated. Again, we attribute this entanglement reduction to the presence of internal loops in the SCNPs. Macromolecular rings indeed experience much fewer contacts with other rings than their linear counterparts of the same molecular weight. This is a consequence of the topological interactions that prevent ring concatenation and lead to depletion of local domains in fractal globular structures.[13,40,41] The entanglements reduction, linked in our case to a lower interpenetration of the chains than for the linear topology, can be considered as an indirect hint of the emergency of a soft-colloidal character in the system.

CONCLUSIONS

In summary, we presented a thorough experimental investigation of the relaxation of a melt fully made of weakly cross-linked SCNPs through a combination of scattering and relaxation techniques highly valuable to probe the complex hierarchy of dynamic processes in this system. No significant impact of intramolecular cross-linking with respect to the linear chains is found for the β- and α-relaxations. A new slow relaxation process emerges at intermediate length scales (∼1 nm), which can be attributed to the heterogeneities provoked by the internal multiloop topology of the SCNPs. A slowly relaxing fraction of the dipolar moment also evidences the impact of internal compartmentation. Thanks to the small fraction of intramolecular cross-links present along the polymer backbone, the melt of SCNPs here investigated develops an intriguing polymer/colloid duality, where internal degrees of freedom play a key role. Due to this duality the rheological properties of this system strongly differ from those of both a 3D network (intermolecular cross-links) and a melt of long linear chains (precursors) without cross-links. Introduction of a small number of intramolecular cross-links leads to a much faster flow than in the reference linear polymer melt. This feature is tentatively assigned to the reduction of intermo-

DOI: 10.1021/acs.macromol.9b01264
Macromolecules 2019, 52, 6935−6942

lecular contacts (and consequently of entanglements) that originates from the characteristic segregation of intramolecular domains in dense systems of loopy objects as rings and more generally SCNPs. Our study thus nicely illustrates the essence of soft materials: "small cause, large effects".[42]

APPENDIX A

Analysis of DS Results

For the precursor, the relaxation curves can be described by a linear superposition of a β- and an α-process plus a power law term to acount for the dc conductivity and other low-frequency effects

$$\varepsilon''(\omega) = \Delta\varepsilon_\beta \mathrm{Im}\{\Phi^*_\beta(\omega)\} + \Delta\varepsilon_\alpha \mathrm{Im}\{\Phi^*_\alpha(\omega)\} + \frac{A}{\omega^k} \tag{A1}$$

For describing the β-relaxation we used a superposition of Debye processes with a log-normal distribution of energy barrier heights,[43,44] which in the frequency domain reads

$$\Phi^*_\beta(\omega) = \int_0^\infty g(E)\frac{1}{1 + i\omega\tau_0 \exp\left(\frac{E}{kT}\right)}\mathrm{d}E \tag{A2}$$

where the distribution function $g(E)$ is taken as

$$g(E) = \frac{1}{\sqrt{2\pi}\sigma_E}\exp\left[-\frac{1}{2}\left(\frac{E - E_0}{\sigma_E}\right)^2\right] \tag{A3}$$

Here σ_E is the width and E_0 is the average of the distribution of activation energies. The values of τ_0 and E_0 are determined from the temperature dependence of the position of the maximum of the relaxation, $\tau = \tau_0 \exp(E_0/kT)$.

Concerning the α−relaxation, we described the relaxation curves by means of the Havriliak−Negami (HN) equation[45]

$$\Phi^*_\alpha(\omega) = \frac{1}{[1 + (i\omega\tau_{HN})^\alpha]^\gamma} \tag{A4}$$

where τ_{HN} is the characteristic relaxation time, and the shape parameters α and γ describe respectively the symmetric and asymmetric broadening of the complex dielectric function and the condition $0<\alpha$; $\alpha\beta \leq 1$ holds. We restricted ourselves to the HN-family functions which describe well the Laplace transform of Kohlrausch−Williams−Watts (KWW) functions.[46] In these cases, the relationships between HN and KWW shape parameters and their characteristic times are[46]

$$\alpha\gamma = \beta^{1.23} \tag{A5a}$$

$$\log\left[\frac{\tau_{\mathrm{HN}}}{\tau_{\mathrm{KWW}}}\right] = 2.6(1 - \beta)^{0.5}\exp(3\beta) \tag{A5b}$$

The best correspondence between the HN and KWW descriptions can be found if the following relation between the HN parameters holds

$$\gamma \approx 1 - 0.8121(1 - \alpha)^{0.387} \tag{A6}$$

For the SCNPs, the shape parameters and relaxation times of the β and α-processes can be fixed to those determined from the precursor analysis. To describe the DS results in this way, we have to presume that only a fraction x_a of the polarization relaxes through the α-process, thus the amplitude of the α-relaxation peak is smaller in the SCNPs. The remaining fraction can be described by a mirrored Cole−Davidson function[47]

$$\Phi^*_{\mathrm{CD}m}(\omega) = 1 - \frac{1}{(1 + (i\omega\tau_{\mathrm{CD}})^{-1})^\gamma} \tag{A7}$$

This way, the imaginary part of the dielectric signal from the SCNPs melt is described by

$$\varepsilon''(\omega) = \Delta\varepsilon_\beta \mathrm{Im}\{\Phi^*_\beta(\omega)\} + \Delta\varepsilon_\alpha[x_a \mathrm{Im}\{\Phi^*_\alpha(\omega)\} + (1 - x_a)\mathrm{Im}\{\Phi^*_{\mathrm{CD}m}(\omega)\}] + \frac{A}{\omega^k} \tag{A8}$$

where the relaxation functions of the β- and α-contributions are fixed from the precursor.

ASSOCIATED CONTENT

Supporting Information

The Supporting Information is available free of charge on the ACS Publications website at DOI: 10.1021/acs.macromol.9b01264.

Raw data and analysis of the dielectric losses of the precursor and SCNP melt; temperature dependence of the x_a and γ-parameters (PDF)

AUTHOR INFORMATION

Corresponding Author

*E-mail: a.arbe@ehu.eus. Phone: +34 943 01 8802.

ORCID

Arantxa Arbe: 0000-0002-5137-4649

Angel J. Moreno: 0000-0001-9971-0763

Present Address

[∇]Centro de Física de Materiales (CFM) (CSIC-UPV/EHU)-Materials Physics Center (MPC), Paseo Manuel de Lardizabal 5, E-20018 San Sebastián, Spain, and IKERBASQUE-Basque Foundation for Science, Maria Diaz de Haro 3, 48013 Bilbao, Spain.

Notes

The authors declare no competing financial interest.

ACKNOWLEDGMENTS

We thank Dr. S. Prévost for his help at D11. The authors gratefully acknowledge the financial support of the Basque Government, code IT-1175-19, and the Ministerio de Economía y Competitividad, code PGC2018-094548-B-I00 (MINECO/FEDER, UE). This work is based on experiments performed at the FOCUS instrument operated by the Swiss Spallation Neutron Source SINQ, Paul Scherrer Institute, Villigen, Switzerland, and has been supported by the European Commission under the seventh Framework Programme through the "Research Infrastructures" action of the "Capacities" Programme, NMI3-II Grant Number 283883.

REFERENCES

(1) In *Single-Chain Polymer Nanoparticles: Synthesis, Characterization, Simulations, and Applications*; Pomposo, J. A., Ed.; John Wiley & Sons: Weinheim, Germany, 2017.

(2) Kröger, A. P. P.; Paulusse, J. M. Single-chain polymer nanoparticles in controlled drug delivery and targeted imaging. *J. Controlled Release* **2018**, *286*, 326−347.

DOI: 10.1021/acs.macromol.9b01264
Macromolecules 2019, 52, 6935−6942

(3) Mavila, S.; Eivgi, O.; Berkovich, I.; Lemcoff, N. G. Intramolecular Cross-Linking Methodologies for the Synthesis of Polymer Nanoparticles. *Chem. Rev.* **2016**, *116*, 878−961.
(4) Altintas, O.; Barner-Kowollik, C. Single-Chain Folding of Synthetic Polymers: A Critical Update. *Macromol. Rapid Commun.* **2016**, *37*, 29−46.
(5) Latorre-Sánchez, A.; Pomposo, J. A. Recent bioinspired applications of single-chain nanoparticles. *Polym. Int.* **2016**, *65*, 855−860.
(6) González-Burgos, M.; Latorre-Sanchez, A.; Pomposo, J. A. Advances in single chain technology. *Chem. Soc. Rev.* **2015**, *44*, 6122−6142.
(7) Lyon, C. K.; Prasher, A.; Hanlon, A. M.; Tuten, B. T.; Tooley, C. A.; Frank, P. G.; Berda, E. B. A brief user's guide to single-chain nanoparticles. *Polym. Chem.* **2015**, *6*, 181−197.
(8) Huo, M.; Wang, N.; Fang, T.; Sun, M.; Wei, Y.; Yuan, J. Single-chain polymer nanoparticles: Mimic the proteins. *Polymer* **2015**, *66*, A11−A21.
(9) Pomposo, J. A. Bioinspired single-chain polymer nanoparticles. *Polym. Int.* **2014**, *63*, 589−592.
(10) Sanchez-Sanchez, A.; Pérez-Baena, I.; Pomposo, J. A. Advances in Click Chemistry for Single-Chain Nanoparticle Construction. *Molecules* **2013**, *18*, 3339−3355.
(11) Moreno, A. J.; Lo Verso, F.; Arbe, A.; Pomposo, J. A.; Colmenero, J. Concentrated solutions of single-chain nanoparticles: a simple model for intrinsically disordered proteins under crowding conditions. *J. Phys. Chem. Lett.* **2016**, *7*, 838−844.
(12) Moreno, A. J; Bacova, P.; Lo Verso, F.; Arbe, A.; Colmenero, J.; Pomposo, J. A Effect of chain stiffness on the structure of single-chain polymer nanoparticles. *J. Phys.: Condens. Matter* **2018**, *30* (3), 034001.
(13) Vlassopoulos, D. Macromolecular topology and rheology: beyond the tube model. *Rheol. Acta* **2016**, *55*, 613−632.
(14) Rubio-Cervilla, J.; Malo de Molina, P.; Robles-Hernández, B.; Arbe, A.; Moreno, A. J.; Alegría, A.; Colmenero, J.; Pomposo, J. A. Facile access to completely deuterated single-chain nanoparticles enabled by intramolecular azide photodecomposition. *Macromol. Rapid Commun.* **2019**, *40* (1−6), 1900046.
(15) Moreno, A. J.; Lo Verso, F.; Sanchez-Sanchez, A.; Arbe, A.; Colmenero, J.; Pomposo, J. A. Advantages of orthogonal folding of single polymer chains to soft nanoparticles. *Macromolecules* **2013**, *46*, 9748−9759.
(16) Gonzalez-Burgos, M.; Arbe, A.; Moreno, A. J.; Pomposo, J. A.; Radulescu, A.; Colmenero, J. Crowding the Environment of Single-Chain Nanoparticles: A Combined Study by SANS and Simulations. *Macromolecules* **2018**, *51*, 1573−1585.
(17) Farago, B. IN11C, medium-resolution multidetector extension of teh IN11 NSE spectrometer at the ILL. *Phys. B* **1997**, *241−243*, 113−116.
(18) Lovesey, S. W. *Theory of Neutron Scattering from Condensed Matter*; Clarendon Press: Oxford, 1984.
(19) Jansen, S.; Mesot, J.; Holitzner, L.; Furrer, A.; Hempelmann, R. FOCUS: a hybrid TOF-sectrometer at SINQ. *Physica B* **1997**, *234−236*, 1174−1176.
(20) Frick, B.; Richter, D.; Ritter, C. Structural changes near the glass transitionâĂŞneutron diffraction on a simple polymer. *EPL (Europhysics Letters)* **1989**, *9*, 557−562.
(21) Arbe, A.; et al. Manuscript in preparation.
(22) Mezei, F.; Knaak, W.; Farago, B. Neutron spin echo study of dynamic correlations near liquid-glass transition. *Phys. Scr.* **1987**, *T19B*, 363−368.
(23) Farago, B.; Arbe, A.; Colmenero, J.; Faust, R.; Buchenau, U.; Richter, D. Intermediate length scale dynamics of polyisobutylene. *Phys. Rev. E: Stat. Phys., Plasmas, Fluids, Relat. Interdiscip. Top.* **2002**, *65* (1−17), 051803.
(24) Khairy, Y.; Alvarez, F.; Arbe, A.; Colmenero, J. Collective features in polyisobutylene. A study of the static and dynamic structure factor by molecular dynamics simulations. *Macromolecules* **2014**, *47*, 447−459.
(25) Novikov, V. N.; Schweizer, K. S.; Sokolov, A. P. Coherent neutron scattering and collective dynamics on mesoscale. *J. Chem. Phys.* **2013**, *138* (1−6), 164508.
(26) Colmenero, J.; Alvarez, F.; Khairy, Y.; Arbe, A. Modeling the collective relaxation time of glass-forming polymers at intermediate length scales: application to polyisobutylene. *J. Chem. Phys.* **2013**, *139* (1−6), 044906.
(27) De Gennes, P.G. Liquid dynamics and inelastic scattering of neutrons. *Physica* **1959**, *25*, 825−839.
(28) Sköld, K. Small Energy Transfer Scattering of Cold Neutrons from Liquid Argon. *Phys. Rev. Lett.* **1967**, *19*, 1023−1025.
(29) Rubinstein, M.; Colby, R. H. *Polymer Physics*; Oxford University Press: Oxford, 2003.
(30) Vogel, H. The law of the relation between the viscosity of liquids and the temperature. *Phys. Z.* **1921**, *22*, 645−646.
(31) Fulcher, G. S. Analysisis of recent measurements of the viscosity of glasses. *J. Am. Ceram. Soc.* **1925**, *8*, 339−355.
(32) Tammann, G.; Hesse, W. Die Abhängigkeit der Viscosität von der Temperatur bie unterkühlten Flüssigkeiten. *Zeitschrift für anorganische und allgemeine Chemie* **1926**, *156*, 245−257.
(33) Lo Verso, F.; Pomposo, J. A.; Colmenero, J.; Moreno, A. J. Multi-orthogonal folding of single polymer chains into soft nanoparticles. *Soft Matter* **2014**, *10*, 4813−4821.
(34) Pomposo, J. A.; Perez-Baena, I.; Lo Verso, F.; Moreno, A. J.; Arbe, A.; Colmenero, J. How Far Are Single-Chain Polymer Nanoparticles in Solution from the Globular State? *ACS Macro Lett.* **2014**, *3*, 767−772.
(35) Arbe, A.; Pomposo, J.; Moreno, A.; LoVerso, F.; González-Burgos, M.; Asenjo-Sanz, I.; Iturrospe, A.; Radulescu, A.; Ivanova, O.; Colmenero, J. Structure and dynamics of single-chain nano-particles in solution. *Polymer* **2016**, *105*, 532−544.
(36) Pomposo, J. A.; Moreno, A. J.; Arbe, A.; Colmenero, J. Local domain size in single-chain polymer nanoparticles. *ACS Omega* **2018**, *3*, 8648−8654.
(37) Das, C.; Inkson, N. J.; Read, D. J.; Kelmanson, M. A.; McLeish, T. C. B. Computational linear rheology of general branch-on-branch polymers. *J. Rheol.* **2006**, *50*, 207−234.
(38) Wang, Z.; Chen, X.; Larson, R. G. Comparing tube models for predicting the linear rheology of branched polymer melts. *J. Rheol.* **2010**, *54*, 223−260.
(39) Ge, T.; Panyukov, S.; Rubinstein, M. Self-Similar Conformations and Dynamics in Entangled Melts and Solutions of Nonconcatenated Ring Polymers. *Macromolecules* **2016**, *49*, 708−722.
(40) Halverson, J. D.; Lee, W. B.; Grest, G. S.; Grosberg, A. Y.; Kremer, K. Molecular dynamics simulation study of nonconcatenated ring polymers in a melt. I. Statics. *J. Chem. Phys.* **2011**, *134* (1−13), 204904.
(41) Rosa, A.; Everaers, R. Ring polymers in the melt state: the physics of crumpling. *Phys. Rev. Lett.* **2014**, *112* (1−5), 118302.
(42) deGennes, P. G.; Badoz, J. *Fragile Objects*; Springer-Verlag, New York, 1996.
(43) Deegan, R. D.; Nagel, S. R. Dielectric susceptibility measurements of the primary and secondary relaxation in polybutadiene. *Phys. Rev. B: Condens. Matter Mater. Phys.* **1995**, *52*, 5653−5656.
(44) Birge, N. O.; Jeong, Y. H.; Nagel, S. R.; Bhattacharya, S.; Susman, S. Distribution of relaxation times in $(KBr)_{0.5}(KCN)_{0.5}$. *Phys. Rev. B: Condens. Matter Mater. Phys.* **1984**, *30*, 2306−2308.
(45) In *Broadband Dielectric Spectroscopy*; Kremer, F., Schönhals, A., Eds.; Springer: Berlin, 2003.
(46) Alvarez, F.; Alegría, A.; Colmenero, J. Interconnection between frequency-domain Havriliak-Negami and time-domain Kohlrausch-Williams-Watts relaxation functions. *Phys. Rev. B: Condens. Matter Mater. Phys.* **1993**, *47*, 125−130.
(47) Böttcher, C. J. F.; Bordewijk, P. *Dielectrics in Time-Dependent Fields*; Elsevier, 1973.

DOI: 10.1021/acs.macromol.9b01264
Macromolecules 2019, 52, 6935−6942